ANALYTICAL STUDY OF HIGHLY TRANSIENT

BASE PRESSURES AT SUPERSONIC SPEEDS

By

HOMER HO TANG

Bachelor of Science

Taiwan Provincial Cheng-Kung University
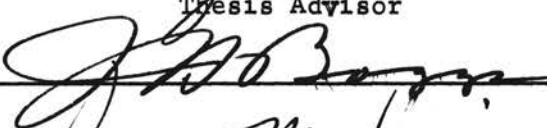
Tainan, Taiwan, Free China

1956

Submitted to the faculty of the Graduate School of
the Oklahoma State University
in partial fulfillment of the requirements
for the degree of
MASTER OF SCIENCE
August, 1961

ANALYTICAL STUDY OF HIGHLY TRANSIENT

BASE PRESSURES AT SUPERSONIC SPEEDS

Thesis Approved:

_____
Thesis Advisor

_____

_____
Dean of the Graduate School

472871

ii

PREFACE

Sincere appreciation is expressed to Dr. Glen W. Zumwalt, an excellent educator, as my thesis advisor, research supervisor and instructor. I am indebted to him for giving me a great deal of his time and effort to direct and improve my study.

I am pleased to have this opportunity to thank Dr. J. H. Boggs, Head of Mechanical Engineering School at Oklahoma State University, for granting the writer a research assistantship. Appreciation is also expressed to Professors Jovanovic, Leonard, Parker, Scholz and Wiebelt, for their generous grants of knowledge.

Thanks also is extended to the Sandia Corporation for a research contract at O.S.U. The idea for this thesis was derived from the frequent activities engaged in by the writer under the program of this research contract.

To my parents in Taiwan, Free China, who, while living in a far place in their old age, have supplied hope and faith, I give my debt of appreciation.

I also appreciate the efforts of Mrs. Claudine King for her careful typing of this manuscript.

Finally, but by no means least, my special thanks goes to my wife, May Shu-I, whose encouragement, patience, and constant care for our infant son, made the writing of this paper possible.

TABLE OF CONTENTS

LIST OF FIGURES

SYMBOLS

a		Sonic velocity
A		Area
B		Dimensionless group defined on page 15
C	$=$	u/u_{max}, Crocco number $= \left(\dfrac{M^2}{\dfrac{2}{K-1} + M^2} \right)^{\frac{1}{2}}$
D		Diameter
erf		Error function, see page 3
f( )		Function of some variables
G_b		Mass rate per unit base width at which air is added to the wake by "bleeding".
G_d		Mass rate added to base region by each mixing stream
h		Base half-height
I_1	$=$	Integral defined on page 15
I_2	$=$	Integral defined on page 15
J_1	$=$	Integral defined on page 15
J_2	$=$	Integral defined on page 15
K		Ratio of specific heats
l		Length of base pressure region
m		Mass flow rate
M		Mach number
P		Absolute pressure
R or r		Radius
$\bar{R}$		Radius of the reference system of coordinates
$\mathcal{R}$		Perfect gas constant
$\mathbb{R}$		A reference streamline near but outside the mixing region

S	Surface area of base pressure region
t	Time
t^{+}	Defined in Equation 6, page 10
T	Absolute temperature
u	Velocity in x or X direction
V	volume
x,y	Coordinates of the intrinsic coordinate system
X,Y	Coordinates of the reference coordinate system
β	Variable in error function
δ	Forebody half angle
Δ	Difference value of two magnitudes
σ	Similarity parameter of the homogeneous coordinate y/x (Also called the free jet spreading parameter)
$\eta = \sigma \frac{y}{x}$	, Dimensionless coordinate
θ	Streamline angle
ρ	Density
$\varphi = $	u/u_2 or u/u_{3a}, Dimensionless velocity, see page 3
ν	Prandtl-Meyer turning angle

Subscripts:

1,2,3,4	Refer to conditions at cross sections indicated in Fig. 1.
a	Refers to conditions of the flow in the isentropic stream adjacent to the dissipative regions.
b	Refers to the conditions at the base of the sudden expansion.
ch	Refers to the chamber of test design.
d	Refers to the streamline whose kinetic energy is just sufficient to enter the recompression region.
f	Refers to conditions after the front oblique shock of the flight vehicle.
j	Refers to conditions along the jet boundary streamline.

m Refers to coordinate shift in the mixing theory due to the momentum integral.

o Stagnation conditions.

ℝ Refers to conditions along the ℝ streamline.

s Refers to conditions to the moving shock.

x Refers to conditions before the transient base pressure occurs.

y Refers to conditions immediately after the transient base pressure begins.

∞ Refers to upstream conditions.

"Prime" Refers to conditions in the transformed plane, see Appendix 2.

CHAPTER I

INTRODUCTION

An analytical study of the interaction of a blast wave and the base pressure region of a missile re-entering the atmosphere is significant for designing anti-missiles. Avenues of approach to this complex problem have been opened by the recent development of jet mixing theories.

Using Korst's (1) theory for base pressures in transonic and supersonic flow, Zumwalt (2), at the University of Illinois, and Beheim (3), at Lewis Research Center, NASA, developed their approximate methods to solve the base pressure problem for axisymmetric configurations.

A research project has been supervised by Dr. Zumwalt of Oklahoma State University and sponsored by Sandia Corporation, and calculations of base pressure-time history were made for two-dimensional and axially-symmetric re-entry bodies, having turbulent flow in the separated boundary layer, when the vehicle passes head-on through a blast wave.

In this thesis, an approximate analysis was performed to predict the response time and geometric requirements for a wind tunnel test to verify the theory as applied to the transient phase of this problem.

CHAPTER II

KORST'S THEORY OF TURBULENT JET MIXING

AND ITS BASE PRESSURE APPLICATION

In 1954, Korst (4) developed a theory for two-dimensional constant pressure turbulent jet mixing, and applied it to the base pressure problem. His basic assumptions were:

(a) two-dimensional backstep

(b) turbulent flow in the mixing region

(c) isoenergetic, constant pressure mixing

(d) exchange-coefficient form for the apparent viscosity relationship.

The essential features of the flow model were:

(a) Prantl-Meyer corner flow at separation

(b) constant pressure jet mixing

(c) an oblique shock in the free stream to define the recompression pressure

(d) the boundary layer at the separation corner as an initial disturbance of the mixing profile, in which, application has been generally made only for the fully developed profile, i.e. for a point far enough downstream that the effect of initial disturbance has been damped out.

If the boundary layer at separation is turbulent and thin compared to the length of the jet mixing region, the base pressure becomes independent of Reynolds number effects. For situations involving base

2

bleed, there is one empirical jet spreading-rate parameter σ, which Tripp (5) suggested as a linear function of the Mach number of the free stream adjacent to the jet mixing zone: $\sigma = 12 + 2.758\ M_2$ (Equation 1).

To derive a turbulent mixing theory, Korst used a flow model, Figure 1, and applied the equation of motion along an "intrinsic" system of coordinates, which system was located in space by its displacement from a corresponding inviscid jet boundary. With this transformation, an asymptotically approached velocity profile was found as $\varphi = \frac{u}{u_2} = \frac{1}{2}(1 + \mathrm{erf}\,\eta)$, where η is a position parameter for the direction normal to the flow and the subscript 2 refers to the free stream adjacent to the mixing region. This asymptotic solution permitted the calculation of the mechanical energy level among the streamlines in the mixing region. We are particularly interested in the streamline, denoted by j, which is separated from the corner of the base, and the streamline, denoted by d, along which the particles just have enough kinetic energy to reach the recompression region. Below d-line, particles will recirculate inside the dead-air region.

In the case of no-bleed into the wake, j and d streamlines are identical. If the wake is fed in, the j streamline has lower velocity than d streamline, and vice versa for feed-out cases. From this, a base pressure could be found without the use of empirical imformation unless mass was being transferred across the mixing region.

The calculation equations may be summed up as follows:

For isoenergetic, fully-developed, turbulent, constant pressure, jet mixing profiles, the velocity ratio is $\varphi = \frac{1}{2}(1 + \mathrm{erf}\,\eta)$, plotted in Figure 3, where $\varphi = \frac{u}{u_2}$, $\mathrm{erf}\,\eta = \frac{2}{\sqrt{\pi}}\int_0^\eta e^{-\beta^2}d\beta$, and $\eta = \sigma\frac{y}{x}$.

As shown in Figure 1, u represents the x component of the velocity in the mixing region, u_2, the free stream x component, x and y the intrinsic coordinates which are displaced from the reference system of coordinates X, Y, that follow the boundary of the corresponding inviscid jet, so that $X \cong x$ and $Y = y - y_m(x)$. The displacement is necessary to satisfy the momentum equation. The symbol σ is the jet spreading parameter, depending upon the free stream Mach No., M_2, or on

$$C_2 = \frac{u_2}{u_2 \, (\text{max.})}.$$

The dimensionless y_m shift is

$$\eta_m = \sigma \frac{Y_m}{X} = \eta_R - \left[1 - C_2^2 \right] \int_{-\infty}^{\eta_R} \frac{\varphi^2}{1 - C_2^2 \varphi^2} \, d\eta$$

where $\quad \left(1 - \varphi(\eta_R) \right) \ll 1$

The location, η_j, of the jet boundary streamline, j, separating the approaching flow from the fluid entrained from the ambient stagnant region is determined by combining momentum and continuity integral equations for the fluid approaching the separation corner. This gives

$$\int_{-\infty}^{\eta_j} \frac{\varphi}{1 - C_2^2 \varphi^2} \, d\eta = \int_{-\infty}^{\eta_R} \frac{\varphi}{1 - C_2^2 \varphi^2} \, d\eta - \int_{-\infty}^{\eta_R} \frac{\varphi^2}{1 - C_2^2 \varphi^2} \, d\eta$$

The mass flow per unit width between the streamlines η_j and η_d is given by

$$G_d = \int_{y_j}^{y_d} \rho u \, dy = \frac{x \, \rho_2 \, u_2 \left[1 - C_2^2 \right]}{\sigma_2} \left[\int_{-\infty}^{\eta_d} \frac{\varphi}{1 - C_2^2 \varphi^2} \, d\eta - \int_{-\infty}^{\eta_j} \frac{\varphi}{1 - C_2^2 \varphi^2} \, d\eta \right]$$

$$= \frac{x \, \rho_{o_2} \left(\frac{K+1}{2} \right)^{\frac{1+K}{2(1-K)}} \left[1 - C_2^2 \right]}{\sigma_2 \sqrt{T_{o_2}} \left. \frac{A}{A^*} \right|_{C_2} \sqrt{\frac{R}{K g_c}}} \left[\int_{-\infty}^{\eta_d} \frac{\varphi}{1 - C_2^2 \varphi^2} \, d\eta - \int_{-\infty}^{\eta_j} \frac{\varphi}{1 - C_2^2 \varphi^2} \, d\eta \right]$$

(Equation 2)

The integrals will be referred to by:

$$I_1(C_2^2, \eta) = \int_{-\infty}^{\eta} \frac{\varphi}{1 - C_2^2 \varphi^2} \, d\eta$$

(Equation 3)

$$I_2(c_2^2, \eta) = \int_{-\infty}^{\eta} \frac{\varphi^2}{1 - c_2^2 \varphi^2} d\eta$$

Values of I_1 and I_2 have been calculated by using a digital computer at the University of Illinois as in Reference 6, and presented in graphical form in Reference 7, I_{1_j} versus c_2^2, and I_1 versus $\dot{c}_2^2$ and φ are plotted in Figure 5(a) and Figure 5(b). I_2 is only used to locate the jet boundary streamline j, and as a parameter to treat the base pressure field for non-isoenergetic situations. Therefore, in our present case, values of I_2 are not specifically required.

CHAPTER III

CALCULATION OF THE BASE PRESSURE-TIME HISTORY

OF A TWO-DIMENSIONAL RE-ENTRY VEHICLE

We here assume a blast wave which consists of a normal shock with
constant conditions following the shock, i.e., a step function.

A. Constant Blast Wave Passing

1). Oblique Shock at Two-Dimensional Wedge: When the supersonic stream
is forced to change direction suddenly, as in a sharp concave corner,
an attached oblique shock occurs and forms a discontinuity. Using
equations of continuity, momentum, and energy, the Rankine-Hugoniot (8)
equation has been derived relating pressures and densities. Prandtl
then developed a relation between the velocity components on two dis-
continuous sides. From these, convenient curves have been plotted by
Dailey and Wood (9) using initial Mach Number and deflection angle as
independent variables. These apply for steady flow.

2). Supersonic Expansion by Turning a Corner: Assuming an isentropic
expansion and extending the linear theory, Prandtl-Meyer derived their
famous function which relates an explicit form of turning angle, $\mathcal{V}$,
with Mach Number, as follows:

$$\mathcal{V}(M) = \int \frac{\sqrt{M^2-1}}{1 + \frac{K-1}{2} M^2} \frac{dM}{M}$$

$$= \sqrt{\frac{K+1}{K-1}} \ Tan^{-1} \sqrt{\frac{K-1}{K+1}(M^2-1)} - Tan^{-1}\sqrt{M^2-1}$$

The constant of integration has been arbitrarily chosen so that $\mathcal{V} = 0$

corresponds to M = 1. Numerical values are available in many publications, e.g. (10).

3). Calculation of Steady Base Pressure: Using Korst's (1), (4), (6), theory, the calculation procedure is as follows for angle of attack = 0:

(a) Pick an arbitrary initial M_2 (Configuration shown in Fig. 1).

(b) Calculate the Crocco Number, $C_2^2 = \dfrac{M_2^2}{\frac{2}{k-1} + M_2^2}$

If K = 1.4 for air, thus, $C_2^2 = \dfrac{M_2^2}{5 + M_2^2}$.

(c) Find φ_j value from Figure 4, φ_j versus C_2^2 curve.

(d) Since Non-Bleed wake flow prevails,

$$\left(\varphi_d\right)^2 = \left(\varphi_j\right)^2 = \left(\frac{u_d/u_{max}}{u_2/u_{max}}\right)^2 = \left(\frac{C_d}{C_2}\right)^2$$

$$\therefore \; C_d^2 = \varphi_j^2 \, C_2^2$$

(e) From isentropic relationships, and $M_2 = M_3$ and $C_2 = C_3$

$$\frac{P_{0_{2d}}}{P_{2d}} = \frac{1}{(1 - C_{2d}^2)^{k/k-1}} = \frac{1}{(1 - C_{2d}^2)^{3.5}} \left(= \frac{P_4}{P_3}\right)$$

(f) Using $\dfrac{P_4}{P_3}$ value from oblique shock chart will give $_3\theta_4$. (9). Assume stream flows from region ① to region ② (Figure 1) by Prandtl-Meyer isentropic turn with the angle $_1\theta_2 = {}_3\theta_4$.

(g) Using Prandtl-Meyer corner flow relation, $\nu_1 = \nu_2 - {}_3\theta_4$ and find M_1. (10). Also find P_1/P_2 from:

$$\frac{P_1}{P_2} = \frac{P_1}{P_0}\bigg|_{M_1} \times \frac{P_0}{P_2}\bigg|_{M_2} \quad \text{using isentropic relations.}$$

(h) So, base pressure P_b is found as,

$$P_b = P_2 = P_1 \times \frac{1}{P_1/P_2}$$

The base pressure ratio P_b/P_1 was plotted on Figure 8, and its calculating procedure is shown in Appendix 1.

4). Moving Blast Wave: In order to deal with the blast wave, which is assumed to travel at constant speed, a relative moving coordinate system is employed, in which the moving wave becomes at rest; and the shock relations already derived are then applicable to the fluid properties in this coordinate system. (8). The same result is true to a very good approximation even when the shock strength is changing with time or when the shock speed is not constant. This is so because the shock thickness is minute, from which it follows that the time rates of change of mass, momentum, and energy within a control surface surrounding the shock are negligible compared with the changes in the respective fluxes of these quantities passing through the control surface. In our case, the blast wave is considered as a normal shock wave passing the body, and referred to as "prime" condition in nomenclature in the transformed plane.

5). Calculation of Base Pressure Just Before (Subscript x) and After (Subscript y) the Shock Front Passes:
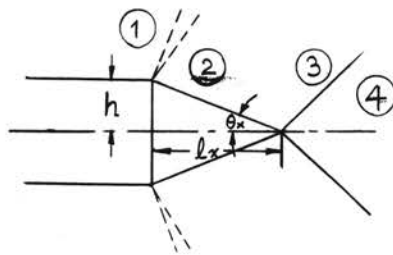
$$\ell_x = \frac{h}{Tan\,\theta_x}$$

$$m_x = \rho\,V_{bx} = \frac{P_{2x}}{R\,T_{bx}} \times \frac{h^2(width)}{Tan\,\theta_x}$$

$$P_{bx} = P_{2x}$$

We use trial and error method to determine the base region situation just after the shock front passes.

Balance $P_{by} = P_{2y}$ by P-M turn and by isentropic compression of the wake.

By isentropic compression of the mass in the wake: $m_{bx} = m_{by}$

and from geometry,

$$\frac{V_y}{(Width)} = h\,\ell_y = \frac{h^2}{Tan\,\theta_y}\,, \quad \text{and} \quad \frac{V_x}{V_y} = \frac{Tan\,\theta_y}{Tan\,\theta_x} = \frac{P_y}{P_x}\frac{T_x}{T_y} = \left(\frac{P_y}{P_x}\right)^{\frac{K-1}{K}}$$

therefore, $\quad P_{by} = P_{bx} \left(\dfrac{Tan\,\theta_y}{Tan\,\theta_x}\right)^{1.4}.$

By Prandtl-Meyer Turn: $\quad P_{2y} = f\,(M_{1y},\ \theta_y)$

Using θ_y as a parameter, a solution which gives P_{by} equal to P_{2y} can be obtained. An example of the calculation procedure has been performed in Appendix 2.

B. Transient Blast Wave Passing

A more realistic blast wave front than that of part A is a shock front behind which the pressure decays. Thus, after the wave passes, transient conditions are impressed.

For any instantaneous flow conditions along the body, a particular steady state base pressure solution can be found. If, due to the transient nature of the flow, the base pressure differs from this, mass will flow into or out of the dead-air region ("wake") to make the base pressure tend toward a stable, i.e., steady-state, condition. This change in pressure due to mass exchange may be opposed or augmented by a pressure change due to the gradually lowering ambient pressure. Thus, base pressure is altered due to its difference from an equilibrium condition and due to a transient impressed pressure field.

1). Mass Transfer into the Wake: Mass added to base region, G_d, by each mixing stream. (11).

$$G_d = -\frac{P_{o1}}{\sqrt{T_o}}\,\frac{c_2(1-c_2^2)^{3.5}}{b_2\,Sin\,\theta}\,\sqrt{\frac{2K}{R(K-1)}}\,(I_j - I_d) \qquad \text{(Equation 4)}$$

The total mass added by upper and lower streams is $2\,G_d$.

$$(\text{mass in wake}) = \rho_b\,V_b = \frac{P_b}{R\,T_o}\times\frac{h^2}{Tan\,\theta}\times(Width)$$

Mass transfer rate, $\frac{dm}{dt}$:

$$\frac{dm}{dt} = 2G_d = \frac{d}{dt}\left(\frac{P_b V_{base}}{R T_b}\right) = \frac{1}{R T_b}\left(P_b \frac{dV_b}{dt} + V_b \frac{dP_b}{dt}\right)$$

if the wake temperature, T_b, is about constant and equal to T_o

Thus, $\quad \dfrac{dP_b}{dt} = \dfrac{2 G_d R T}{V_b} - \dfrac{P_b}{V_b}\dfrac{dV_b}{dt} = \dfrac{P_b G_d}{\frac{1}{2}(\text{mass in wake})} - \dfrac{P_b}{\left(\frac{h^2}{Tan\theta}\right)}\dfrac{d\left(\frac{h}{Tan\theta}\right)}{dt}$

$$\cong \frac{P_b G_d}{\frac{1}{2}(\text{mass in wake})} - \frac{\left(\frac{Tan\theta_t}{Tan\theta_{t+\Delta t}} - 1\right)P_b}{\Delta t} \qquad \text{(Equation 5)}$$

2). Trial and Error Solution for Base Pressure: Assume a value, choose a small time interval Δt, which will give us

$P_{b_{t+\Delta t}} = P_{b_t} + \dfrac{dP_b}{dt}\Delta t \quad$ and $P_{\infty_{t+\Delta t}}$ by an empirical blast relation. For a blast wave, it was suggested by Sandia Corporation that

$$\Delta P_t = \Delta P_{max}\left(1 - \frac{t}{t^+}\right)e^{-\frac{t}{t^+}} \qquad \text{(Equation 6)}$$

where t^+ is shown on the following figure, and can be obtained from Sandia Corporation publications. (17).
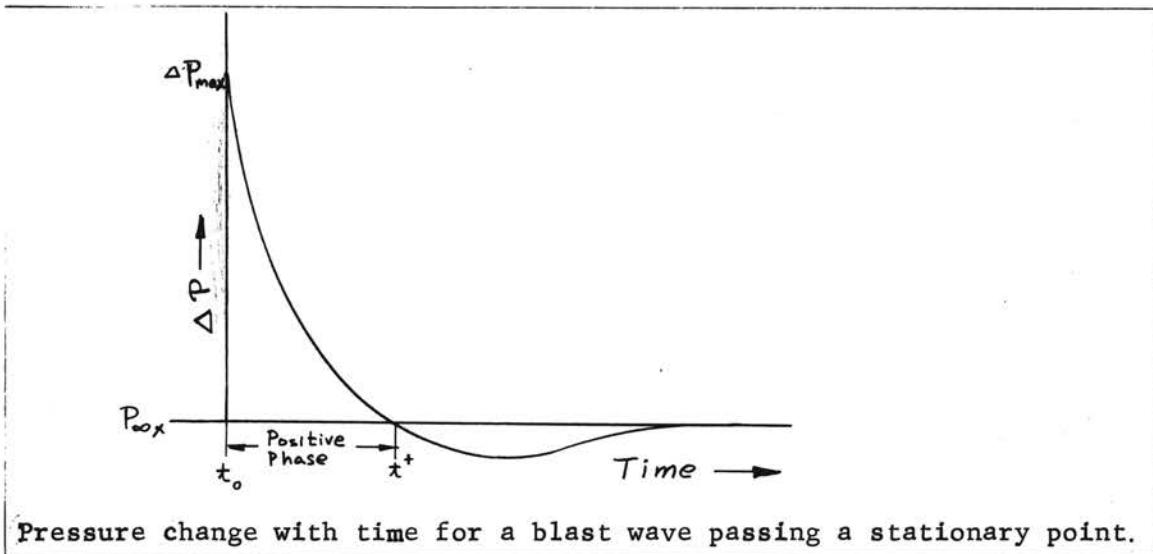
Pressure change with time for a blast wave passing a stationary point.

Since, $P_{\infty_{t+\Delta t}} = P_{\infty_x} + \Delta P$, we can find $Tan\,\theta_{t+\Delta t}$ by the calculation method outlined previously, and therefore can check our assumption for $Tan\,\theta_t / Tan\,\theta_{t+\Delta t}$. The problem can be solved by iteration. An example of calculating procedure is shown in Appendix 3.

The results of Mach number equals 2, at the altitude of 20,000 ft., and blast strength of 100 kt are plotted in Figure 9, 10, and 11, where ΔP_{max} is used as a parameter.

CHAPTER IV

BASE PRESSURE OF AXISYMMETRIC CONFIGURATION

A. Introduction

Dealing with axisymmetric configurations, a particular complica-
tion arises in that the coalescing trailing shock would vary with dis-
tance from the test body because of the complicated interference of
the three dimensionality of the flow. Close to the test-body surface,
it would be approximately two-dimensional in character; and at suf-
ficiently large distances, it would be nearly conical. Thus, an addi-
tional consideration would be required. Due to the difficulty in
theoretical approach, several approximate methods have been developed
based on systematic studies, (i.e., experiments). The following two
methods have been introduced.

B. Zumwalt's Method

Zumwalt (2) tried to solve the axisymmetric base pressure problems
with two separate treatments, one for internal expanding jets and the
other for external jet boundaries.

1). Internal Expanding Jets: For flow inside axially symmetric walls,
Zumwalt concluded that:

   (a) The use of two-dimensional expansion at the separation corner
        is satisfactory.

   (b) The assumption of jet mixing at constant pressure is experi-

mentally verified.

(c) The potential flow solution for obtaining the "corresponding inviscid jet boundary" as a reference system of coordinates is useable.

(d) The two-dimensional error function velocity profile for mixing is still advisable.

(e) The use of the oblique shock recompression, based on the adjacent free stream flow, leads to serious discrepancies with actual, measured recompression pressures. Also, the isentropic recompression process for the discriminating streamline appears generally to be too stringent an assumption. An empirical expression for the effective pressure rise ratio was derived from experimental data.

Since in this present thesis, only the external flow has been considered, the internal flow cases will be omitted.

2). External Jet Boundary Flow:

Concepts and Conclusions:

Dealing with external flow past axially symmetric bodies having sudden reductions in diameter, Zumwalt (2) reached the following conclusions:

(a) The use of two-dimensional expansion at the separation corner is satisfactory, unless boundary layer thickness is appreciable, in which case a modification was presented as a "lip-shock". (12).

(b) The assumption of constant pressure mixing cannot be maintained, as may be seen from results obtained using that assumption. (Figure 7). Instead, the potential flow past a

cone is utilized for defining the pressure field impressed on the mixing region.

This conclusion is due to two substantiating types of evidence. One, Schlieren pictures from many sources show cone-like streamlines after suddenly-terminated bodies of revolution. And two, E. S. Love (12) measured the pressure in the wake at axial locations and found these to be very similar to the pressures on a cone-tail.

(c) The cone, as utilized in (b) above, also serves as the "corresponding inviscid jet boundary". Since a pressure gradient exists along the streamlines, further modification of the flow can be expected. These effects will be evaluated later.

(d) The use of the error function velocity profile proved advantageous. Area (radius) effects due to axial-symmetric flow are considerable and were determined by analytical means. Some detailed descriptions are presented in the next section, Analysis of the Jet Mixing Region With Pressure Rise.

(e) The oblique shock recompression was used in calculations in conjunction with the procedures outlined above. Agreement with published experimental data on sting-supported cylinders was satisfactory and showed marked improvement over the previous attempts to apply two-dimensional mixing theory directly.

Analysis of the Jet Mixing Region with Pressure Rise: (Figure 2).

Defining the coordinate systems in the same way as Korst (1), Zumwalt (2) added two more considerations. One, the pressure change along the mixing region is the same as that along a conical surface coinciding with the "corresponding inviscid jet boundary", and the pressure

gradient normal to the "corresponding inviscid jet boundary" is zero within, and in the vicinity of, the mixing region. And two, the velocity of the jet adjacent to the mixing region is that which would prevail along the conical "corresponding inviscid jet boundary". He wrote the momentum equation in the axial direction with some geometrical and reference coordinate transformation and solved simultaneously with the combined viscid and inviscid continuity equations between the separation corner cross-section, section 2, and a downstream flow cross-section 3, for the mass passing along the annular stream tube bounded by streamlines j and a large value of $\eta_{R}(=3)$. Finally, he got the governing equation as follows:

$$(B-3)^2 + 2(1-C_{3a}^2)\left[I_1\Big|_{-\infty}^{3} - I_1\Big|_{-\infty}^{\mathscr{D}_j}\right]B - 2(1-C_{3a}^2)\left(J_1\Big|_{-\infty}^{3} - J_1\Big|_{-\infty}^{\mathscr{D}_j}\right) = \left(\frac{5\,\overline{R}}{x\cos\theta}\right)_3^2$$

where

$$B = \frac{J_1\Big|_{-\infty}^{\mathscr{D}_j} - \left(1-\frac{C_{3a}}{C_{2a}}\right)J_1\Big|_{-\infty}^{3} - \frac{C_{3a}}{C_{2a}}(J_1-J_2)\Big|_{-\infty}^{3}}{I_1\Big|_{-\infty}^{\mathscr{D}_j} - \left(1-\frac{C_{3a}}{C_{2a}}\right)I_1\Big|_{-\infty}^{3} - \frac{C_{3a}}{C_{2a}}(I_1-I_2)_{-\infty}^{3} - \frac{K-1}{K}\frac{3}{C_{2a}C_{3a}}\left(1-\frac{P_2}{P_3}\right)}$$

I_1, I_2, J_1, and J_2 are integrals which are functions of C_{3a}^2, and the working curves of these were plotted in Figures 7, 8, 9, and 10. (2). The subscript "a" represents flow adjacent to the mixing region for base with pressure rise condition.

To give some physical understanding of the above equation, note that $\overline{R}$ is the radius of the mixing region and thus introduces the axisymmetric aspect into the solution. If $\overline{R} \rightarrow \infty$, this reduces to the two-dimensional solution.

C. Beheim's Method

Beheim (3) in interpreting a series of experimental tests at Lewis

Research Center, Cleveland, Ohio, assumed that, for axisymmetric config-
urations such that the base pressure ratio is less than 1.0, the free
streamline is one of constant pressure. For a cylinder with sudden re-
duction in radius, this jet boundary streamline curves toward the axis.
As the smaller cylinder's radius is decreased, the constant-pressure
flow must approach it at an increasing angle. But there is a limit to
the turning angle which can be obtained by a trailing shock. Therefore,
he suggested that it is possible that a minimum effective radius ratio
exists and that base pressure is independent of test-body geometric
radius ratio for values less than this minimum.

The experimental data shows that the minimum wake radius ratio was
between 0.4 and 0.5, where his theoretical calculations show a minimum
radius ratio of about 0.55. At these regimes, the trailing shock pres-
sure rises were very close to the plane shock value. Thus, Beheim (3)
suggested using the minimum wake radius ratio of 0.5 and solving the
trailing shock pressure ratio with a plane shock recompression.

CHAPTER V

EXPERIMENTAL INVESTIGATION

A. Objectives

Since there is no exact theoretical solution for the base pressure field in axisymmetric configurations, the objectives of this chapter are to investigate an approximate analytical method to estimate the response time and prescribe the geometric requirements for a wind tunnel test to verify the validity of the mixing theory's application to axisymmetry.

B. Theoretical Considerations

For wind tunnel tests, a real blast wave may be difficult to produce. In order to verify our approximate calculation method, a different type of transient condition will be generated. A low pressure (1.57 psia) air chamber with a diaphragm-closed end is provided. This forms the afterbody of the model, with the diaphragm at the base. When the diaphragm is burst, the pressure of the base is suddenly lowered and creates a transient state similar to that of a base after a sudden blast wave has passed the base. Since this evaluates only the transient phase of a blast wave, the sudden pressure rise phase must be tested separately. Tests of instrumented rockets flying through high-explosive blasts are being devised separately to investigate this effect. Only the transient tests will be dealt with here.

1). **Base Conditions Before Diaphragm Burst;** (Subscript x)

$$T_{bx} \cong T_{\infty x}$$
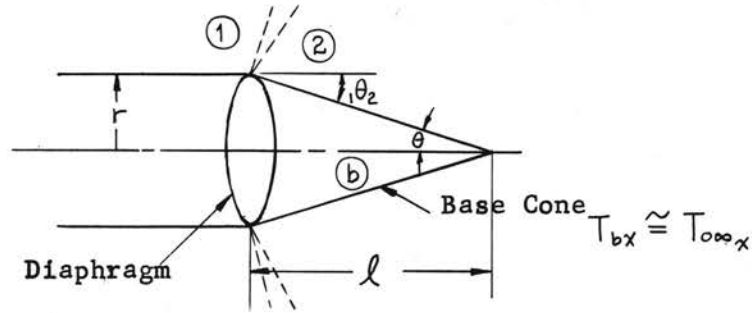
volume of air in the base cone, V_{bx}

$$V_{bx} = \frac{1}{3}\pi r^2 \ell_x = \frac{\frac{1}{3}\pi r^3}{\tan\theta_x}$$

mass of air in base cone, m_{bx}

$$m_{bx} = \rho V_{bx} = \frac{P_{2x}}{R T_{bx}} \frac{\pi}{3} \frac{r^3}{\tan\theta_x}$$

2). **Base Conditions Immediately After Diaphragm Burst:** (Subscript y)

Assuming instantaneous equilibrium when the diaphragm bursts, since the air in the base cone has no velocity relative to the body, it expands into the chamber:

$$m_{chy} + m_{by} = m_{chx} + m_{bx}$$

where,

$$m_{chy} = \frac{P_{by} V_{ch}}{R T_{chy}} \quad ; \quad m_{by} = \frac{P_{by} V_{by}}{R T_{by}}$$

$$m_{chx} = \frac{P_{chx} V_{ch}}{R T_{chx}} \quad ; \quad m_{bx} = \frac{P_{bx} V_{bx}}{R T_{bx}}$$

$$T_{bx} = T_{chx} = T_o$$

$$T_{chy} = T_o \left(\frac{P_{by}}{P_{chx}}\right)^{\frac{K-1}{K}} \quad ; \quad T_{by} = T_o \left(\frac{P_{by}}{P_{bx}}\right)^{\frac{K-1}{K}}$$

therefore, $\dfrac{P_{by} V_{ch}}{R T_o (P_{by}/P_{chx})^{(K-1)/K}} + \dfrac{P_{by} V_{by}}{R T_o (P_{by}/P_{bx})^{(K-1)/K}} = \dfrac{P_{chx} V_{ch}}{R T_o} + \dfrac{P_{bx} V_{bx}}{R T_o}$

or, $V_{ch}\left[P_{by}\left(\dfrac{P_{chx}}{P_{by}}\right)^{\frac{K-1}{K}} - P_{chx}\right] = V_{bx}\left[P_{bx} - \dfrac{V_{by}}{V_{bx}}P_{by}\left(\dfrac{P_{bx}}{P_{by}}\right)^{\frac{K-1}{K}}\right]$ (Equation 7)

where, $\dfrac{V_{by}}{V_{bx}} = \dfrac{(1/3)\pi r^3 (1/\tan\theta_y)}{(1/3)\pi r^3 (1/\tan\theta_x)} = \dfrac{\tan\theta_x}{\tan\theta_y}$.

3). **Mass Transfer in the Mixing Region:**

As the flow approaches the axis in the axisymmetric configuration, two things occur:

(a) The flow width circumferentially for the j and d streamlines grows smaller. Thus, G_d would tend to be less than the two-dimensional equation shown in Chapter III, due to reduction in flow area $[(y_j-y_d)2\pi r_{local}$, where r_{local} tends to small value].

(b) The mixing region thickens to satisfy continuity equation. Thus, $(y_j - y_d)$ should increase.

Apparently, (a) and (b) should off-set each other. Accordingly, using the figure shown below,
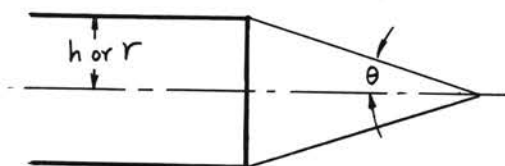
base pressure response rate is proportional to mass addition per unit volume of dead-air space, G_d/V. Mass inflow depends on the size of the jet mixing surface, that is, G_d/S tends to be the same for all configurations under similar imposed conditions.

The volume to mixing-surface ratios of base regions are:

For two-dimensional wakes,

$$\frac{V}{S} = \frac{(h^2/Tan\theta)\ell}{(2h/Sin\theta)\ell} = \frac{h}{2}(Cos\,\theta)_{two-dim.}$$

where h is the half-height of the base, and

$$\frac{G_d}{V} = \frac{G_d}{S}\frac{S}{V} = \frac{G_d}{S}\frac{2}{h(Cos\,\theta)_{two-dim.}}\cdot$$

For axisymmetric wakes,

$$\frac{V}{S} = \frac{\frac{\pi r^3}{3\,Tan\theta}}{\frac{r}{Sin\theta}\frac{r}{2}2\pi} = \frac{r}{3}(Cos\,\theta)_{axi-sym.} \quad \therefore \quad \frac{G_d}{V} = \frac{G_d}{S}\frac{3}{r(Cos\,\theta)_{axi-sym.}}.$$

Since $(Cos\,\theta)_{two-dim.}$ is less than $(Cos\,\theta)_{axi-sym.}$, G_d/V and V/S for two-dimensional cases are about the same values as G_d/V and V/S for axisymmetric cases. Thus, it is suggested to adopt the form of "G_d" equation in Chapter III for two-dimensional cases to be used in axisym-

metric configurations as:

$$G_d = -\frac{P_{o1}}{\sqrt{T_o}} \frac{2\pi r^2}{\sin\theta} \frac{C_2(1-C_2^2)^{3.5}}{\bar{b}_2} \sqrt{\frac{2K}{R(K-1)}} (I_j - I_d)$$

(Equation 8)

Let us consider the blast wave and cylindrical body problem, with the additional chamber volume in the test design.

mass in the wake, m_{wake} is

$$m_{wake} = \rho V = \frac{P_2}{R T_o} \frac{1}{3} \frac{\pi r^3}{\tan\theta}$$

mass transfer rate, $\frac{dm}{dt}$:

$$\frac{dm}{dt} = G_d = \frac{d}{dt}\left(\frac{P_b V}{R T_o}\right) = \frac{1}{R T_o}\left(P_b\frac{dV}{dt} + V\frac{dP_b}{dt}\right)$$

$$\left(G_d R T_o - P_b\frac{dV}{dt}\right)\frac{1}{V} = \frac{dP_b}{dt} = G_d\frac{RT}{V} - \frac{P_b}{V}\frac{dV}{dt}$$

where,

$$\frac{RT}{V} = \frac{P_b}{\text{mass in Conical Wake + Chamber}} = \frac{P_b}{m_{wake+ch}}$$

and V = total volume of base and chamber (subscript, ch) as present design.

so

$$\frac{dP_b}{dt} = \frac{G_d P_b}{m_{wake+ch}} - \frac{P_b}{\frac{\pi}{3}\frac{r^3}{\tan\theta}+V_{ch}}\left[\frac{1}{3}\pi r^3\frac{d\left(\frac{1}{\tan\theta}\right)}{dt}\right]$$

or, in finite difference form:

$$\frac{\Delta P_b}{\Delta t} = \left[\frac{G_d}{m_{wake+ch}} - \frac{\frac{1}{3\tan\theta_t}\frac{\tan\theta_t}{\tan\theta_{t+\Delta t}}-1}{\left(\frac{1}{3\tan\theta_t}+\frac{V_{ch}}{\pi r^3}\right)\Delta t}\right]\cdot P_b$$

(Equation 9)

In the same manner as Chapter III, a trial and error solution can be performed by assuming a particular value of $\tan\theta_t / \tan\theta_{t+\Delta t}$ and balancing the base pressure by isentropic compression and by Prandtl-Meyer expansion. For the isentropic compression, as for blast passage, the pressure relation can be derived. Assuming $T_{by} \cong T_{o\infty y}$, we can write an equation for mass balance of the air trapped in the base region.

$$m_{by} = \frac{P_{2y}}{R T_{by}}\frac{\pi}{3}\frac{r^3}{\tan\theta_y} = m_{bx} = \frac{P_{2x}}{R T_{bx}}\frac{\pi}{3}\frac{r^3}{\tan\theta_x}$$

or,

$$\frac{P_{2y}}{T_{by}}\frac{1}{\tan\theta_y} = \frac{P_{2x}}{T_{bx}}\frac{1}{\tan\theta_x}$$

isentropic relation gives,

$$\left(\frac{T_{by}}{T_{bx}}\right) = \left(\frac{P_{2y}}{P_{2x}}\right)^{\frac{K-1}{K}}$$

$$\frac{P_{zy}}{P_{zx}} = \left(\frac{P_{2y}}{P_{2x}}\right)^{\frac{K-1}{K}} \frac{Tan\,\theta_y}{Tan\,\theta_x}$$

or

$$\frac{P_{2y}}{P_{2x}} = \left(\frac{Tan\,\theta_y}{Tan\,\theta_x}\right)^{K} \qquad\qquad \text{(Equation 10)}$$

It is noted that this result is the same as a two-dimensional wake.

C. Apparatus and Calculations:

1). Test Design:
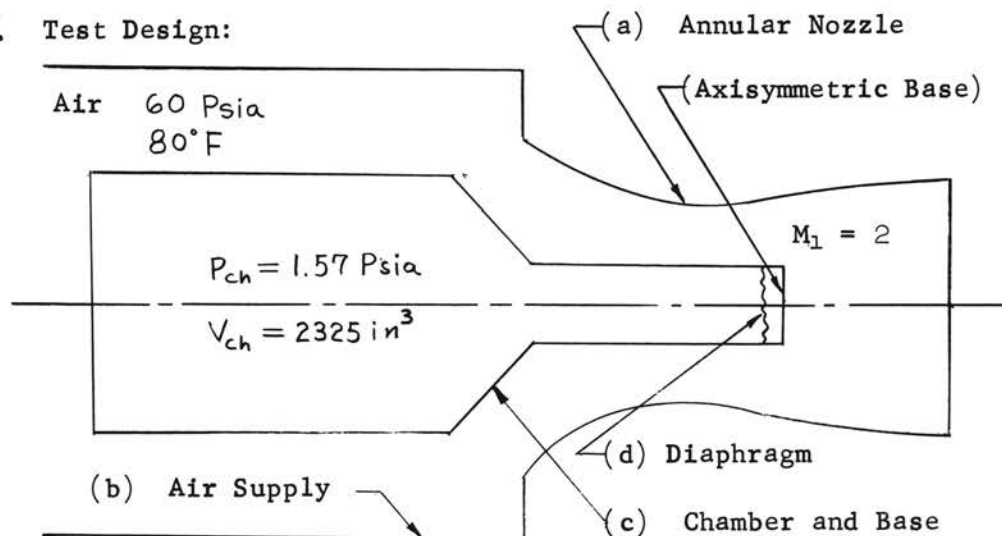
For detail dimensions, see Figure 12. The principal items required are as follows:

(a) Annular Nozzle: Coordinates shown in Figure 13. (13)

(b) Air Supply: A supply of air at stagnation pressure 60 psia and stagnation temperature 80°F, and air flow rate of 38.98 lbm/sec for at least 20 seconds.

(c) Chamber and Base: Evacuate to pressure of 1.57 psia. Total

volume = 2325 in^3, see Part 3).

3" diameter annular base.

(d) **Diaphragm:** capable of being punctured remotely.

2). **Base Pressure Before Diaphragm Burst:** (14) $\frac{P_{bx}}{P_1} \cong .622$, $P_1 = 7.77$ psia
therefore, $P_{bx} = .622 \times 7.77 = 4.769$ Psia

$$\frac{P_{bx}}{P_o} = \frac{4.769}{60} = .07949 \rightarrow 34.38, \therefore \theta_2 = \nu_2 - \nu_1 = 34.38 - 26.38 = 8°$$

3). **Base Pressure Immediately After Diaphragm Burst:** Calculation of total volume of chamber, V_{ch}. See Figure 12.

$$V_{ch} = \frac{\pi}{4}(11.5)^2 \times 19.75 + \frac{1}{3} \times \frac{\pi}{4}\left[2.625^2 + 11.5^2 + 2.625 \times 11.5\right] \times 4.25$$
$$+ \frac{\pi}{4}(2.625)^2 \times 16 = 2050.3 + 188.3 + 86.5 = 2325 \text{ in}^3$$

Since $\quad \pi r^3 = \pi(1.3125)^3 = 7.1031 \text{ in}^3$

$$\therefore \quad V_{ch} = \frac{2325}{7.1031}\pi r^3 = 327.32\,\pi r^3$$

$$V_{bx} = \frac{1}{3}\pi r^3 \frac{1}{\tan\theta_x} = 2.372\,\pi r^3$$

From Equation 7, we have:

$$V_{ch}\left[(P_{by})^{\frac{1}{1.4}}(P_{chx})^{\frac{1}{3.5}} - P_{chx}\right] = V_{bx}\left[P_{bx} - \frac{\tan\theta_x}{\tan\theta_y}(P_{by})^{\frac{1}{1.4}}P_{bx}^{\frac{1}{3.5}}\right]$$

or $\quad 327.32\left[P_{by}^{\frac{1}{1.4}} \times 1.137 - 1.57\right] = 2.372\left[4.77 - \frac{0.1405}{\tan\theta_y}(P_{by})^{\frac{1}{1.4}} \times 1.57\right]$

or $\quad P_{by} = \left(\frac{1}{0.7086 + \frac{0.00099}{\tan\theta_y}}\right)^{1.4}$ (Equation 11)

from the Prandtl-Meyer expansion relation,

$$\nu_2 = (26.38° + \theta_y) \rightarrow P_{2y} = P_{by} \qquad \text{(Equation 12)}$$

Solving equations 11, 12 simultaneously, we obtain

$$\theta_y = 23.24° \quad \text{and} \quad P_{by} = 1.64 \text{ Psia}$$

4). **Pressure Rise at "End of the Wake" by oblique shock:** Characteristic free jet boundary results show that the $_3\theta_4$ is variable. (15). See Figure 1. It is suggested by Beheim (3) to use r/R = 0.5 to get the angle $_3\theta_4$ from characteristic results for constant pressure jet boundaries. (15). We can continue, however, to an acceptable degree of accuracy, to calculate the base air volume by conical wake geometry.

5). Calculation Procedure: Basic equations: Equations 8 and 9.

(1). t, choose increments of time.

*(2). P_b, (2) previous value + (e) x (34) previous calculation. (e) = Δt.

(3). P_b/P_{01}

(4). M_2, (3) $\rightarrow$ (4) by isentropic relation. (10).

(5). ν_2, (4) $\rightarrow$ (5) by Prandtl-Meyer relations. (10).

(6). $_1\theta_2$, (5) $\rightarrow \nu_1$

(7). $\sin_1\theta_2$

(8). $\tan_1\theta_2$

(9). c_2^2, (4)^2/5 + (4)^2

(10). I_j, (9) $\rightarrow$ (10) from Figure 5

(11). $_3\theta_4$, (15).

(12). P_4/P_2, (M_2 and $_3\theta_4$) $\rightarrow P_4/P_3$ by oblique shock curves. (9).

(13). c_d^2, $1 - \dfrac{1}{(12)^{.286}}$

(14). ϕ_d, $\sqrt{(13)/(9)}$

(15). I_d, [(9) and (14)] $\rightarrow$ (15) from Figure 5

(16). P_{01}, given

(17). $\sqrt{T_{01}}$, given

(18). 2.758 x (4)

(19). $\bar{b}_2$, $12 + $ (18) by Tripp's equation (5).

(20). C_2, $\sqrt{(9)}$

(21). $1 - c_2^2$, $1 - $ (9)

(22). $(1 - c_2^2)^{3.5}$, (21)$^{3.5}$

(23). G_d/ft. of base length, (16) x (20) x (22) / (12) x (19) x (7)

(24). $I_j - I_d$, (10) $-$ (15)

_____

* Initial value is P_{by} as found in 3).

25 . $G_d/2\pi r^2$, $-296.1 \times$ ㉓ $\times$ ㉔ , where $296.1 = 144 \sqrt{\dfrac{2K}{R(K-1)}}$

26 . $1/3 \ Tan_1\theta_2$, $1/3$ ⑧

27 . $(V_{ch}/\pi r^3) +$ ㉖

28 . mass in wake/πr^3, $144 \times$ ㉗ $\times$ ② $/$ ⑰$^2 \times R$

29 . G_d/mass in wake, 2 ㉕ $/r \times$ ㉘

30 . $\dfrac{Tan_1\theta_2}{Tan(_1\theta_2)_{t+\Delta t}}$

31 . $\dfrac{\dfrac{Tan_1\theta_2}{Tan(_1\theta_2)_{t+\Delta t}} - 1}{\Delta t}$, $\dfrac{㉚ - 1}{\Delta t}$

32 . $\dfrac{\dfrac{1}{3 \ Tan_1\theta_2} \times \dfrac{\dfrac{Tan_1\theta_2}{Tan(\theta_2)_{t+\Delta t}} - 1}{\Delta t}}{\dfrac{V_{ch}}{\pi r^3} + \dfrac{1}{3 \ Tan_1\theta_2}}$, $\dfrac{㉖ \times ㉛}{㉗}$

33 . $(G_d$/mass in wake$) -$ ㉜ ,   ㉙ $-$ ㉜

34 . $\Delta P_b/\Delta t$, ㉝$\times$ ②

CHAPTER VI

CONCLUSIONS AND SUGGESTIONS

A. Axisymmetric Results

Calculation results of Chapter V are shown in Figure 14. The
approximate time, in our case, is about 0.4 seconds for P_b to become
essentially equal to P_b stable. At that time, $_1\theta_2$ is about 8° and
$(I_j - I_d)$ is about zero, that is, conditions are identical with the
beginning steady conditions. This result verified the accuracy of our
step-by-step calculations.

The author regrets that there are no experimental data available
at present due to the time schedule of the research contract in which
the author is participating. This thesis is then limited to theoret-
ical evaluation only.

B. Suggestions For Further Study

1). The validity of the simplified theoretical method is expected to
be experimentally evaluated by the test described in this thesis. It
is suggested that these tests be performed and the analytical method
reviewed in the light of the test results.

2). The transient base pressure of a flight vehicle due to a moving
blast wave is affected by transient atmospheric condition for a finite
period of time. A wholly reliable picture can be obtained only by
actual flight testing with full scale models and blasts. Such blasts

are presently prohibited by international agreement.

3). The wind tunnel test can be run for several steady state conditions using base bleed rate as a parameter. Results of these will be helpful when plotted as P_b versus G_b with a given outside flow condition. Thus, we may have a better ability to determine the effective base bleed surface instead of utilizing the unproven models used in previous theories.

4). The empirical equation for free jet spreading parameter, σ , suggested by Tripp (5), rests on a very poor foundation. This linear relation between σ and Mach number was derived by passing a straight line through the available data points, shown in Figure 6. This data is grouped around two Mach number regions, 0 and 1.7. The linear form is thus only a conjecture. Also, the data are strictly applicable only to two-dimensional jets, and may be expected to become inaccurate when the mixing width of an axisymmetric jet is an appreciable fraction of the radius.

Therefore, experimental work is badly needed to determine the σ values as functions of Mach number and mixing width to radius ratio. Suggestions for this have been made to Sandia Corporation and the Aerophysics Division is planning to perform measurements to evaluate the spreading parameter for Mach numbers 0.7, 1.0, 1.5, and 2.0. Plans are being made for Mach 3.0 test at O.S.U. All these will utilize pitot and static pressure surveys at various axial stations of constant pressure circular jets to permit calculation of velocity profiles and thus of σ .
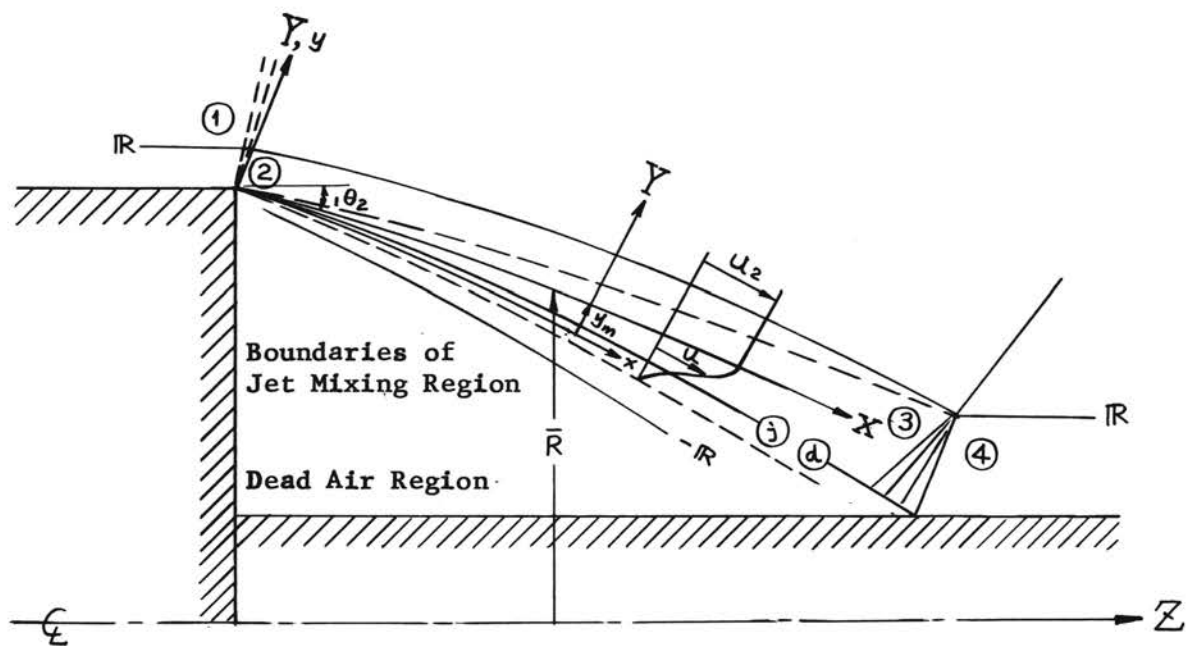
FIGURES

Figure 1. Model for the Constant Pressure Jet Mixing Analysis
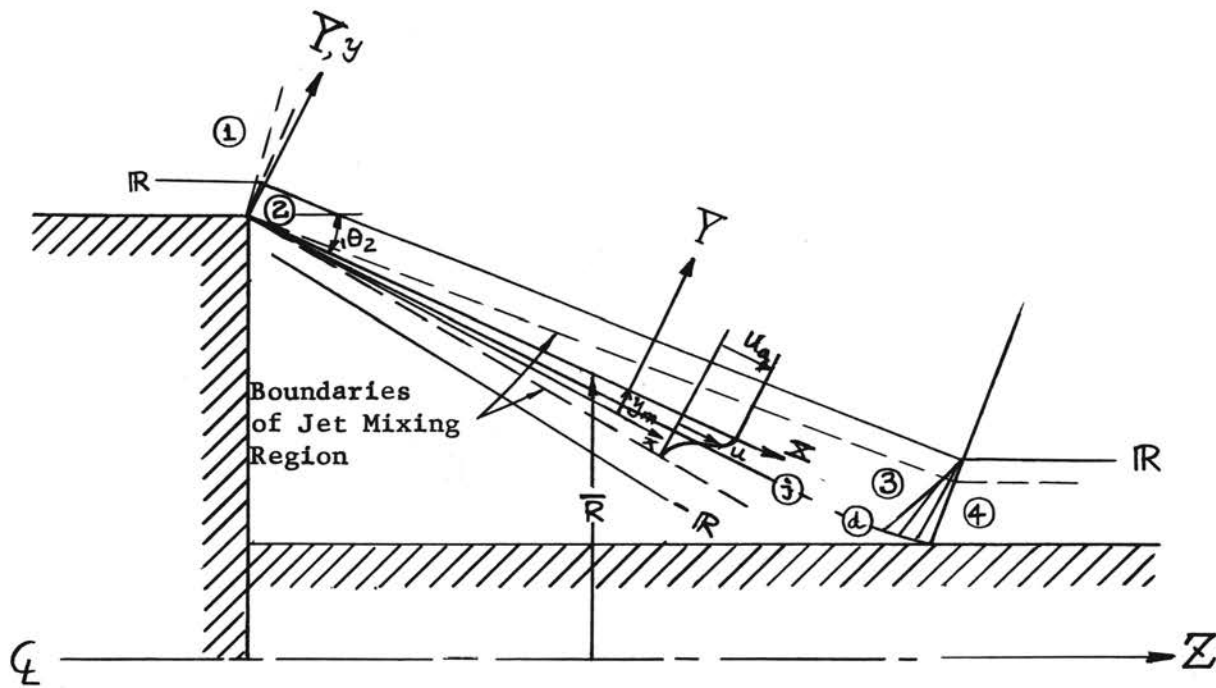
Figure 2. Flow Model For Use in The Analysis of a Free Jet Boundary
     With Rising Pressure.
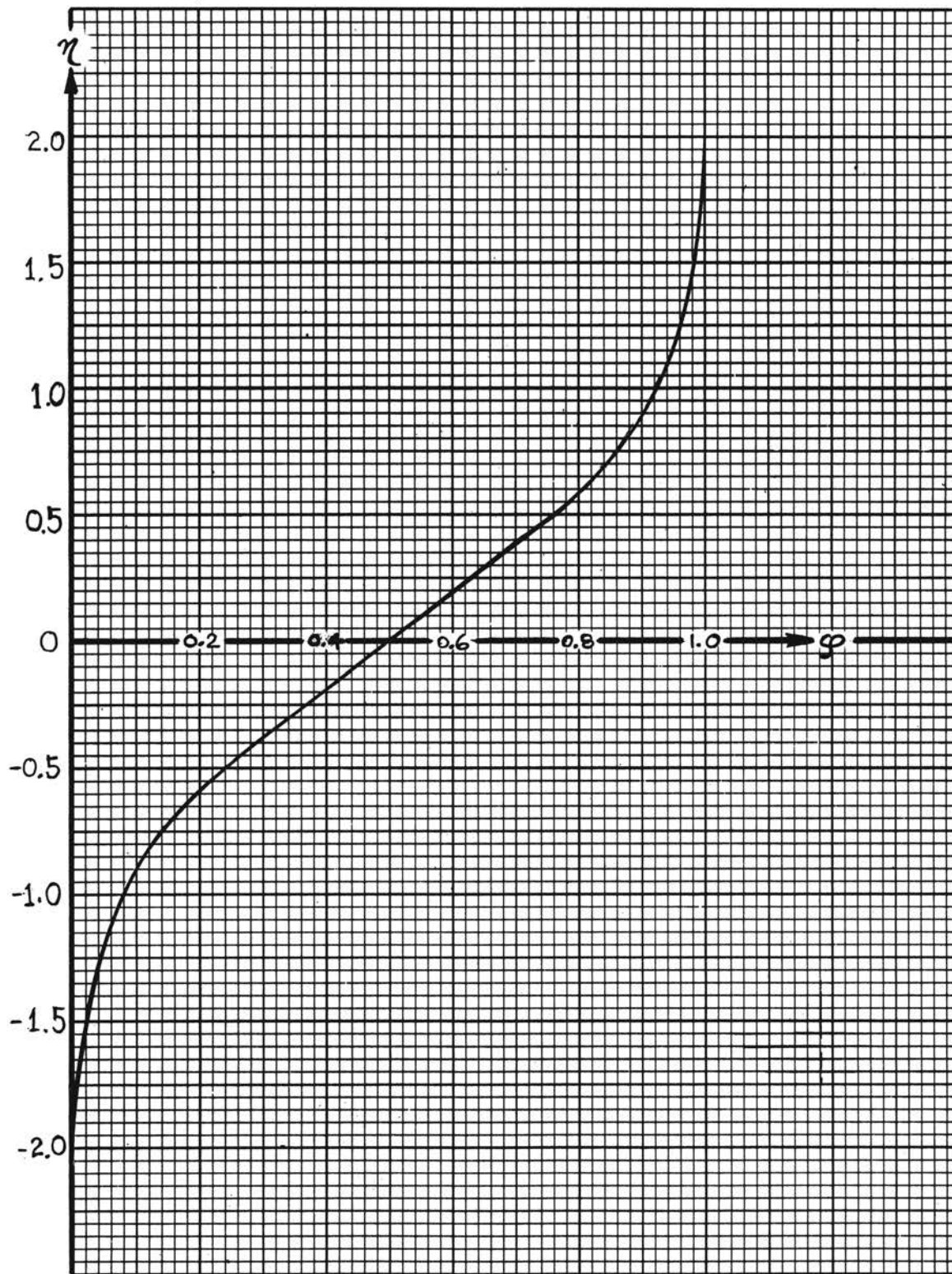
Figure 3. Dimensionless Velocity φ As A Function of η
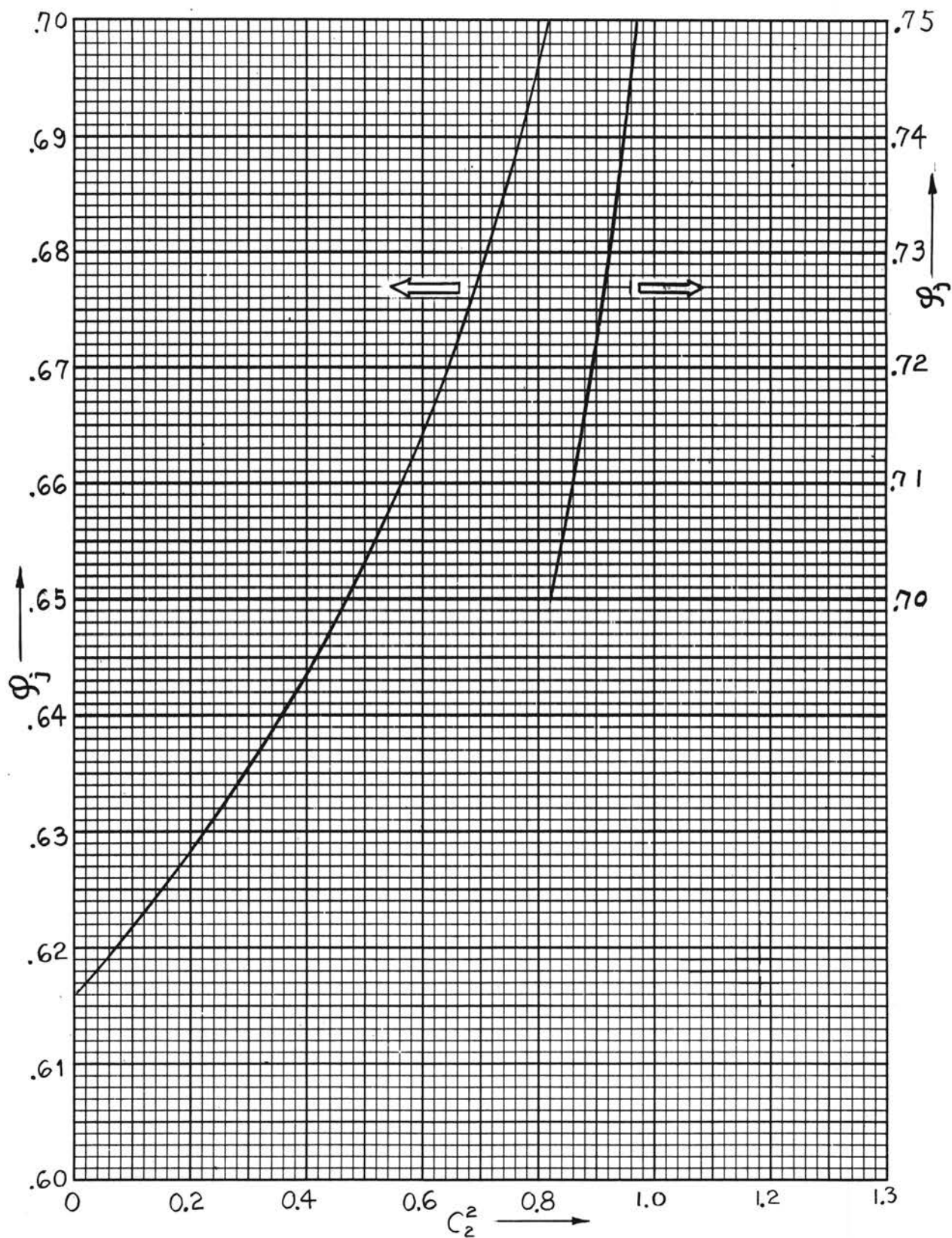
Figure 4. Two-Dim. Jet Mixing φ_j vs C_2^2
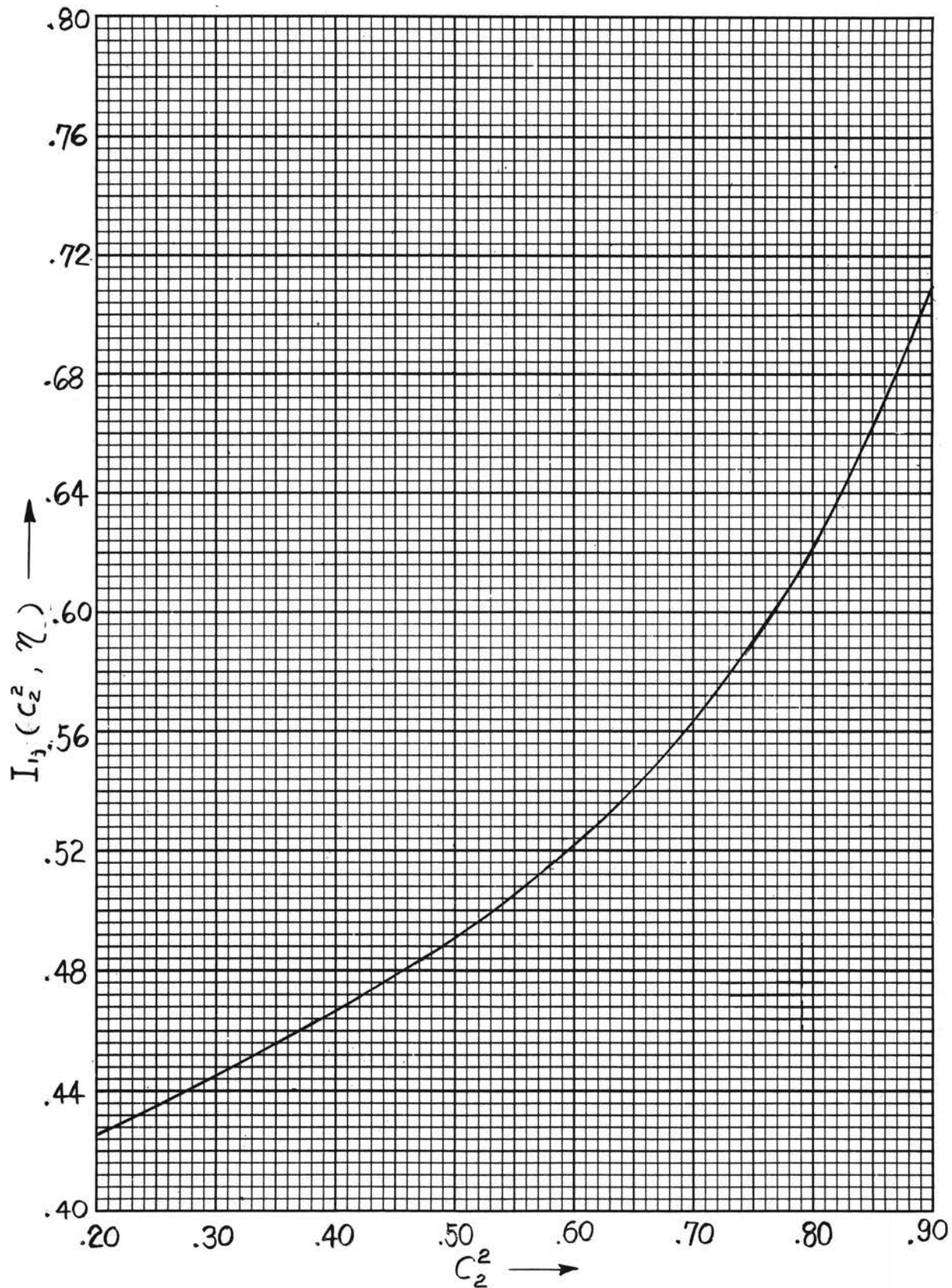
Figure 5(a). Plot of I_{1j} Integral for the Error Function Profile
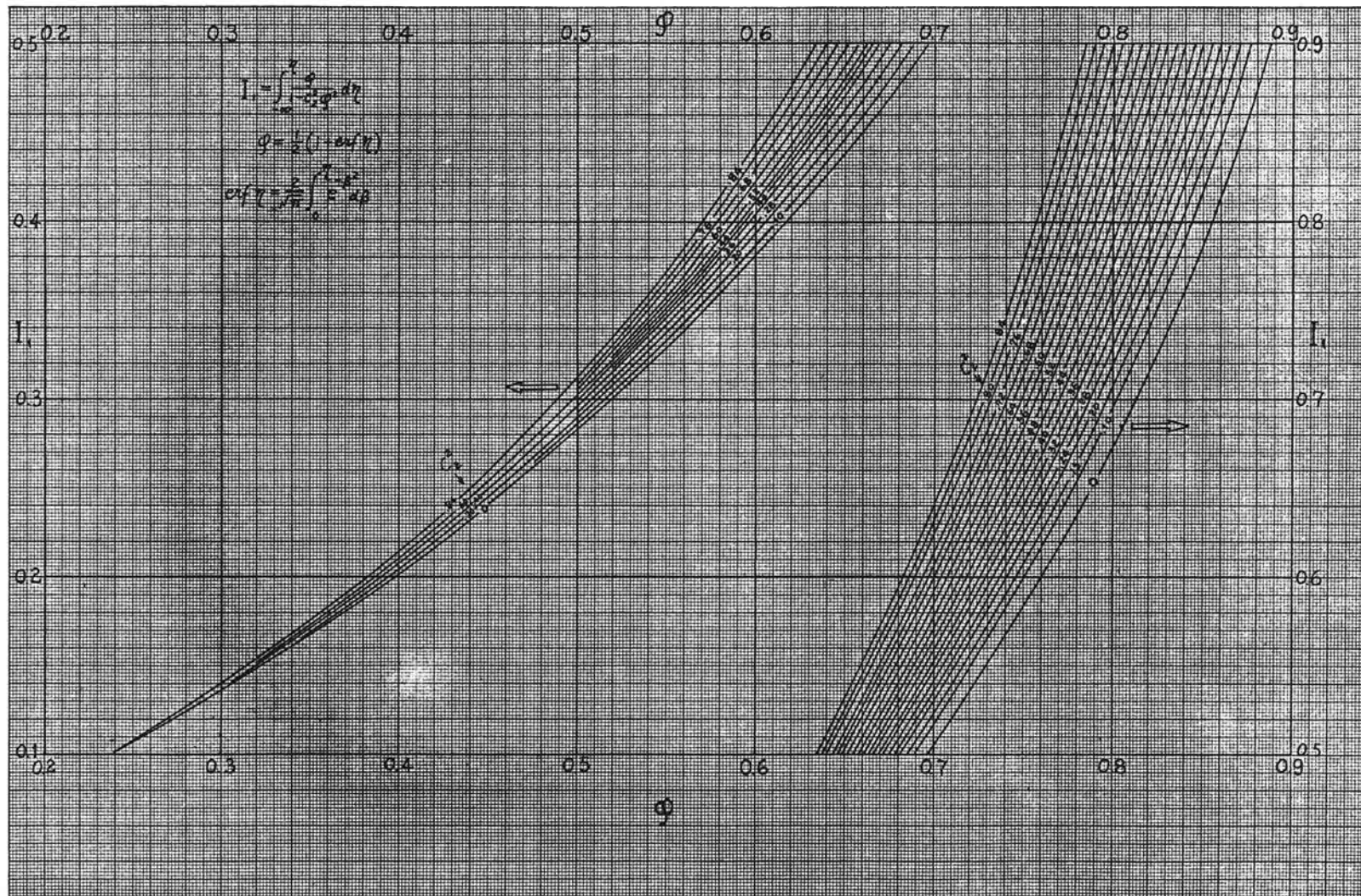
Figure 5(b). Plot of the I_1 Integral for the Error Function Profile.
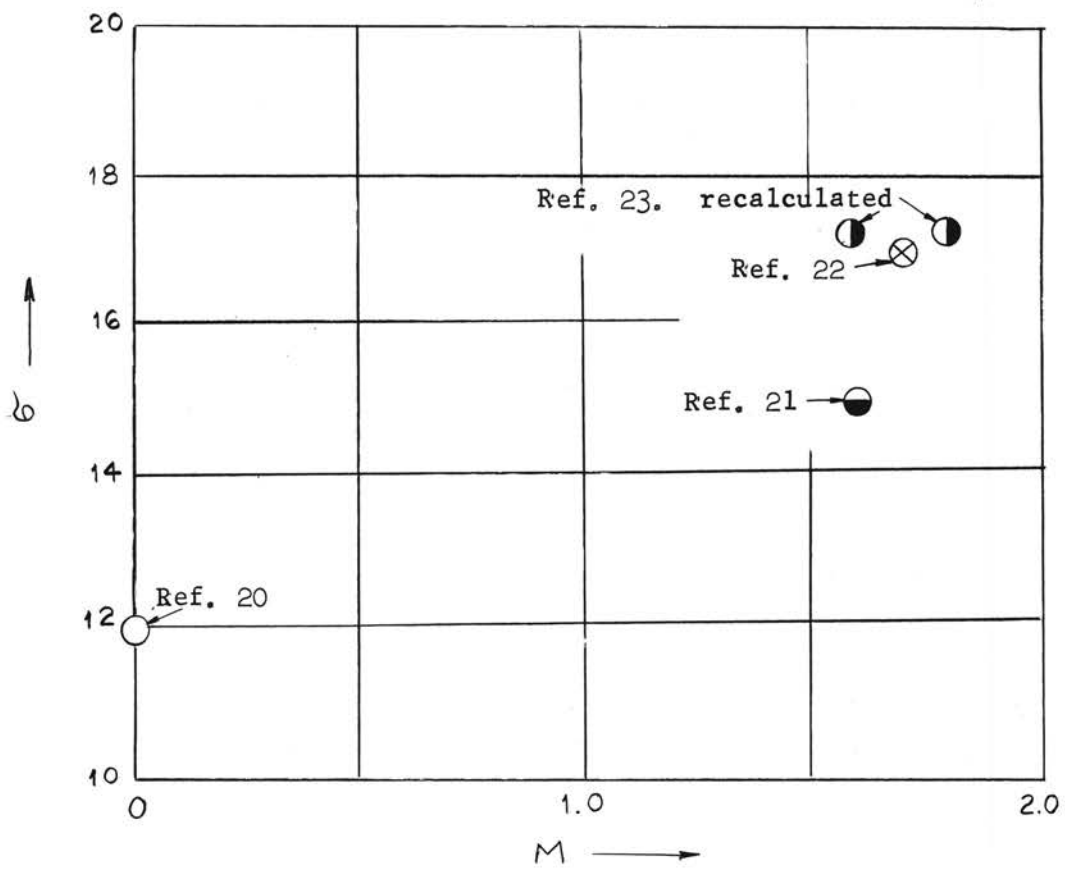
Figure 6. Experimentally Observed Values of Free Jet Spreading Parameter, 6.
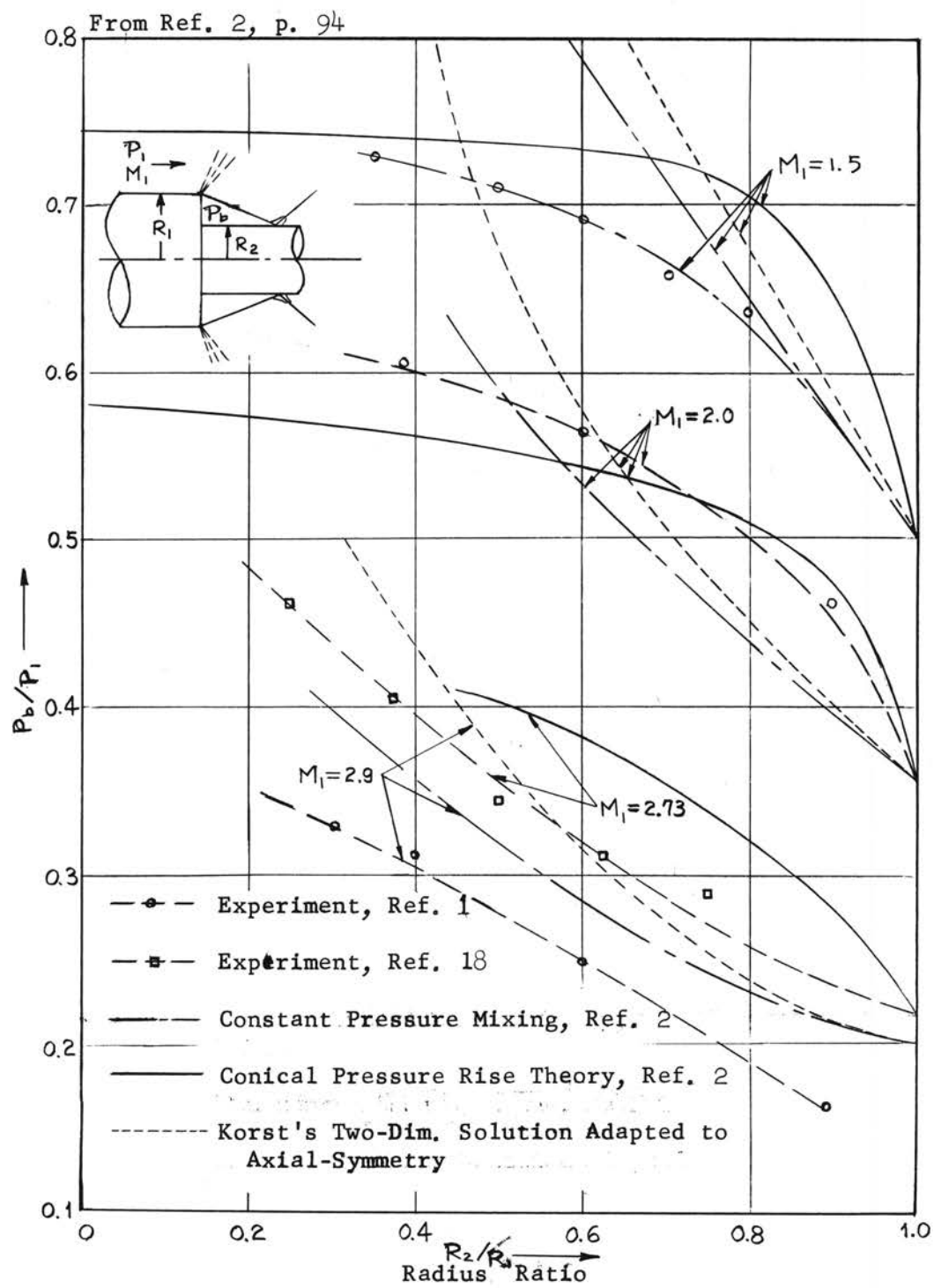
Figure 7. Comparison of the Conical Flow Theory With Experiment For External Flow Past a Cylinder with Reduced Radius.
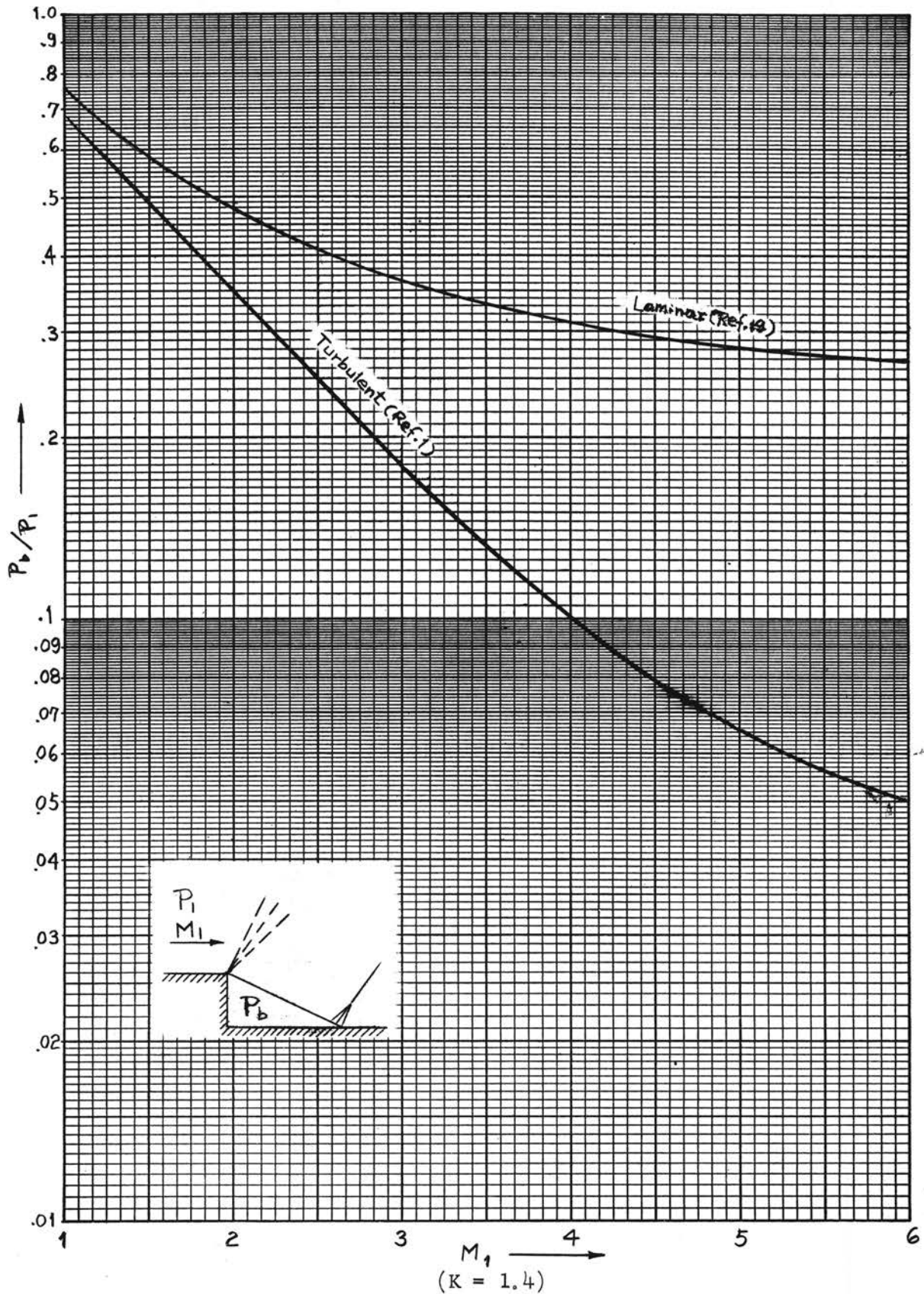
Figure 8. Two-Dim. Base Pressure Ratio
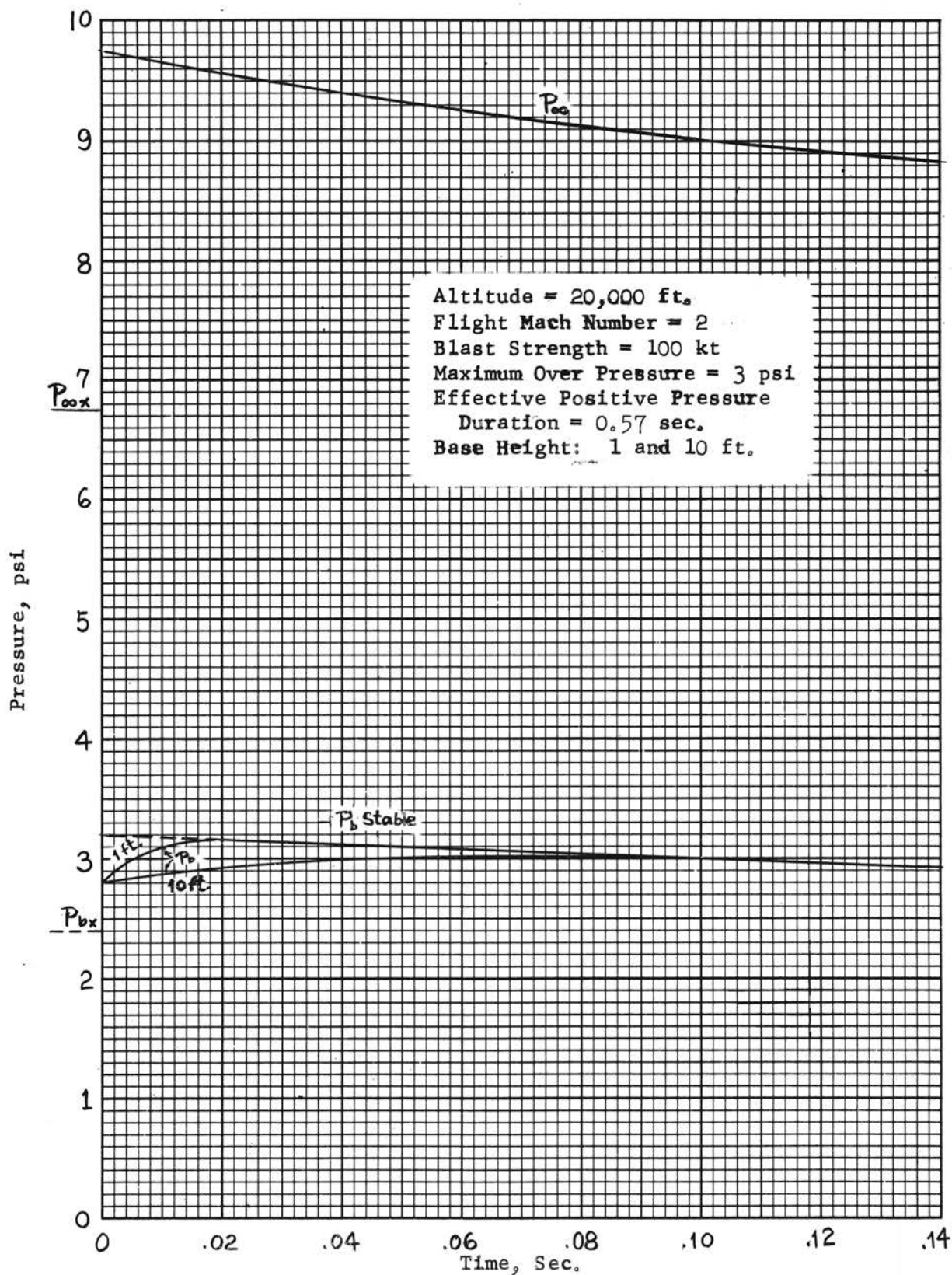
Figure 9. Time History of Two-Dim. Transient Base Pressure

Figure 10. Time History of Two-Dim. Transient Base Pressure
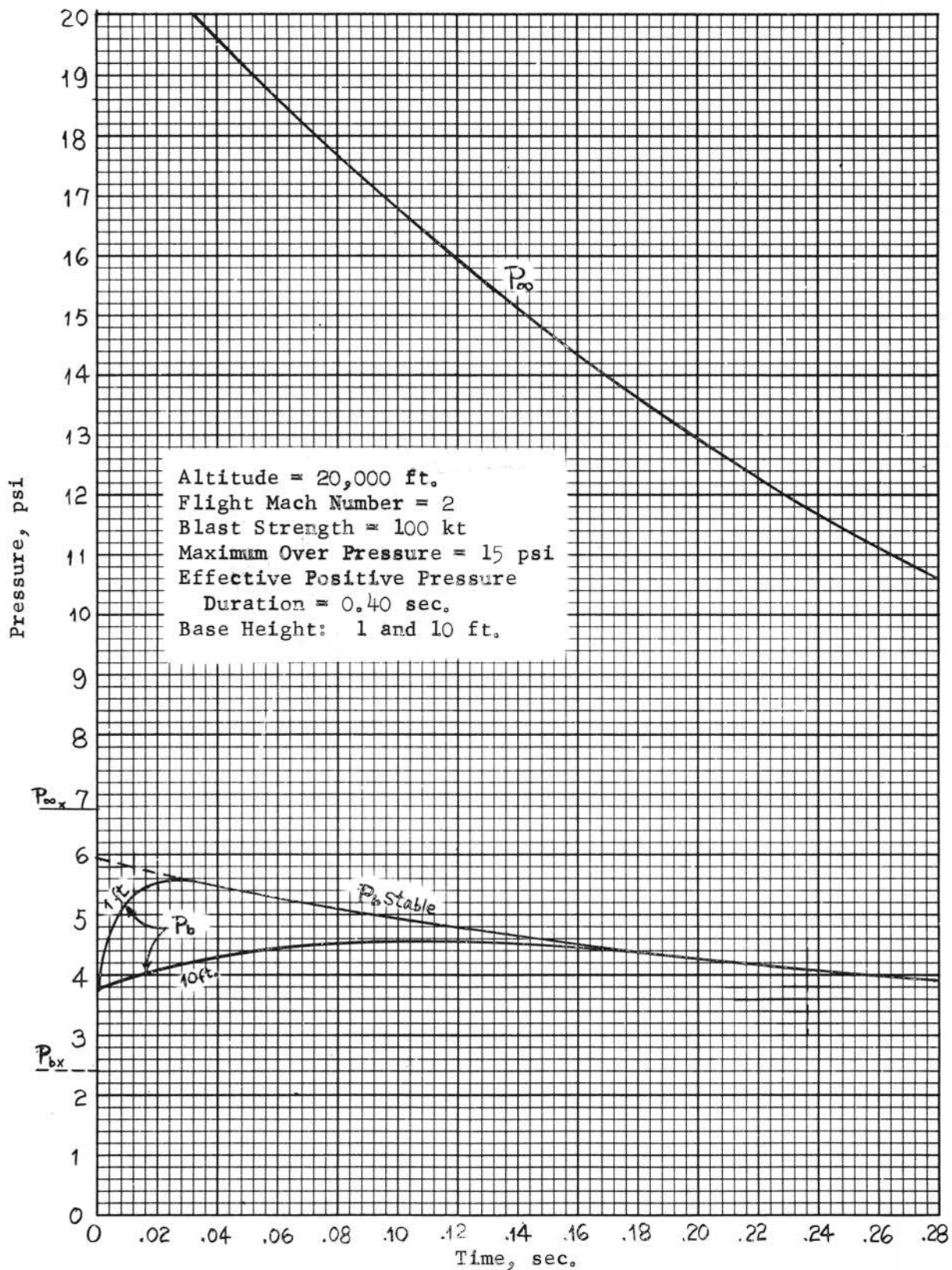
Figure 11. Time History of Two-Dim. Transient Base Pressure

☒ Pressure Transducer

〰️ Diaphragm

Approx. 12" O.D. 11.5" I.D.

45°

3" O.D. 2.625" I.D. (Approx.)

½"

16"

4"

20"

4.25"

1"

Note:
Center body must be exactly
centered and aligned with
axis.
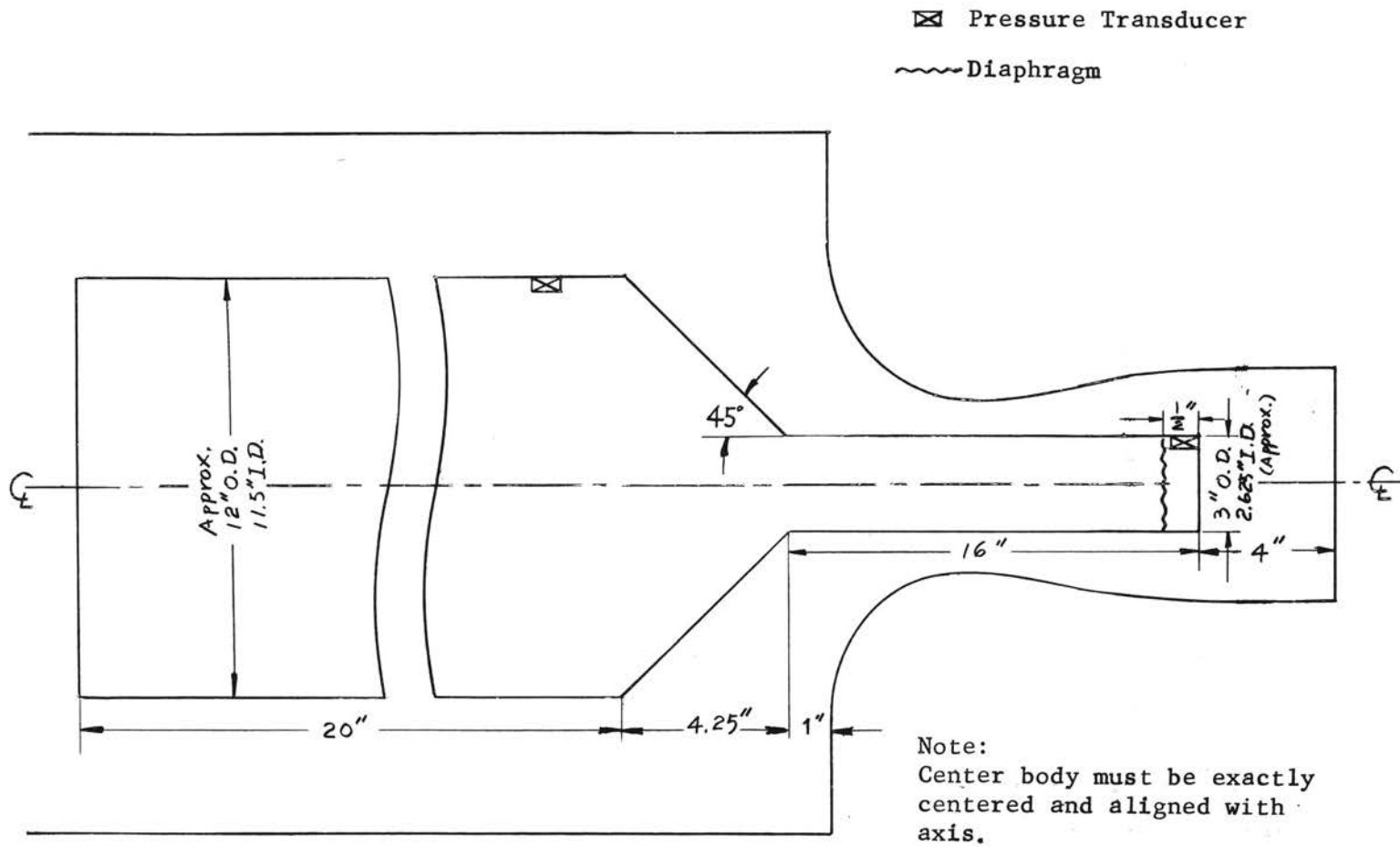
Figure 12. Model Configuration For Annular Nozzle Test of Transient Base Pressure

From Ref. 13
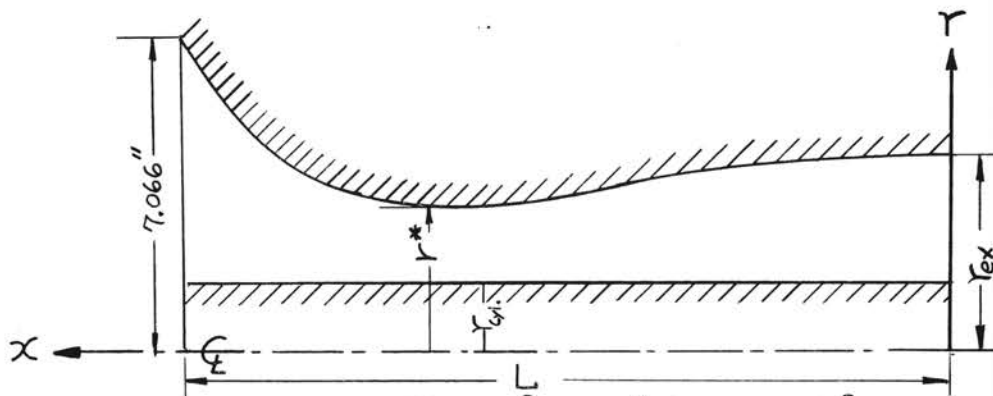
$K = 1.40$
$r^* = 3.374"$
$r_{ex} = 4.240"$
$r_{cyl} = 1.5"$
$L = 16.73"$

$A^* = \pi \left[(3.374^2 - 1.5^2)\right] = 28.7 \text{ in}^2$
Mass Flow for Stagnation Conditions of 60 psia and 80°R is,

$$\dot{m} = 0.532 \frac{P_0 A^*}{\sqrt{T_0}} = 0.532 \frac{60 \times 28.7}{23.5} = 38.98 \text{ lbm/sec.}$$

x	r	x	r	x	r	x	r
0.0	4.240	3.4	4.142	6.8	3.874	10.2	3.434
0.2	4.238	3.6	4.134	7.0	3.850	10.4	3.414
0.4	4.236	3.8	4.124	7.2	3.824	10.6	3.398
0.6	4.232	4.0	4.114	7.4	3.798	10.8	3.386
0.8	4.228	4.2	4.102	7.6	3.772	11.0	3.378
1.0	4.224	4.4	4.090	7.8	3.746	11.18	3.374*
1.2	4.220	4.6	4.078	8.0	3.720	11.98	3.426
1.4	4.216	4.8	4.064	8.2	3.692	12.78	3.522
1.6	4.210	5.0	4.050	8.4	3.664	13.18	3.614
1.8	4.204	5.2	4.034	8.6	3.636	13.58	3.730
2.0	4.198	5.4	4.018	8.8	3.608	13.98	3.872
2.2	4.192	5.6	4.000	9.0	3.580	14.38	4.042
2.4	4.186	5.8	3.982	9.2	3.554	14.78	4.250
2.6	4.178	6.0	3.962	9.4	3.528	15.18	4.502
2.8	4.170	6.2	3.942	9.6	3.504	15.58	4.810
3.0	4.162	6.4	3.920	9.8	3.480	15.98	5.208
3.2	4.154	6.6	3.898	10.0	3.456	16.26	5.574
						16.73	7.066

*Throat

Figure 13. Mach 2 Annular Nozzle Co-ordinates
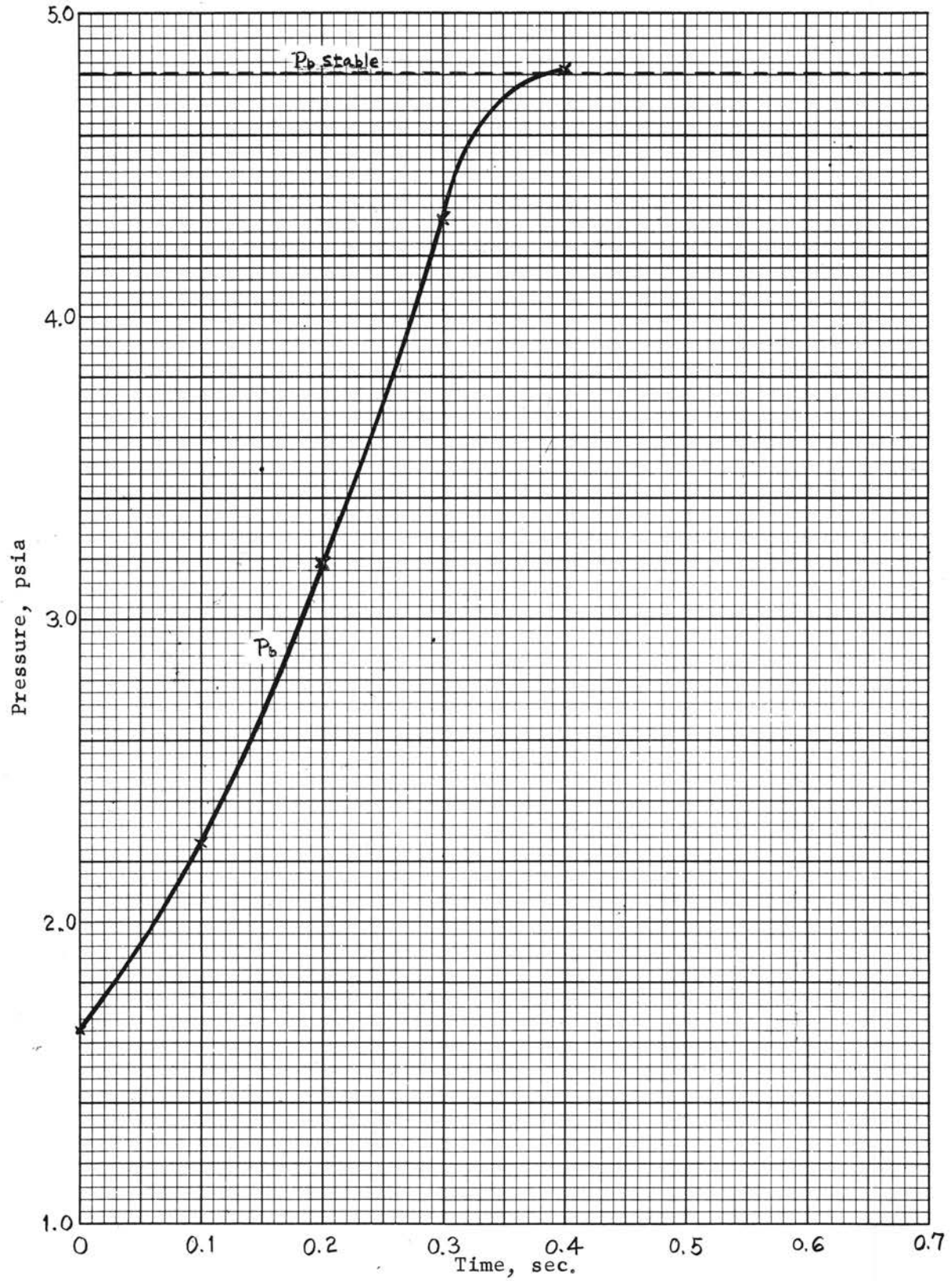
Figure 14. Results of Calculation of Wind Tunnel Test Situation.

SELECTED BIBLIOGRAPHY

1. Korst, H. H., Page, R. H., and Childs, M. E. A Theory for Base Pressures in Transonic and Supersonic Flow. Univ. of Illinois, ME-TN-392-2, OSR-TN-55-89, Contract No. AF 18(600)392, March 1955.

2. Zumwalt, G. W. Analytical and Experimental Study of the Axially-Symmetric Supersonic Base Pressure Problem. Ph.D. Dissertation, Univ. of Illinois, 1959.

3. Beheim, M. A. Flow in the Base Region of Axisymmetric and Two-Dimensional Configurations. Lewis Research Center, NASA-TR-R-77, 1960.

4. Korst, H. H., Page, R. H., and Childs, M. E. Compressible Two-Dimensional Jet Mixing at Constant Pressure. Univ. of Illinois, ME-TN-392-1, OSR-TN-54-82, Contract No. AF 18(600)392, April, 1954.

5. Tripp, Wilson, Analytical and Experimental Investigation of the Base Pressure Behind a Blunt Trailing Edge for Supersonic Two-Dimensional Flow. (Approaching streams have same stagnation temperatures, but different Mach numbers and stagnation pressures). Ph.D. Thesis, Univ. of Illinois. June 1956.

6. Korst, H. H., Page, R. H., Childs, M. E. Compressible Two-Dimensional Jet Mixing at Constant Pressure Tables of Axialiary Functions for Fully Developed Mixing Profiles. Univ. of Illinois, ME-TN-392-3, OSR-TN-55-99, Contract No. AF 18(600)32, April 1955.

7. Korst, H. H., and Chow, W. L., Compressible Non-Isoenergetic Two-Dimensional Turbine Jet Mixing at Constant Pressure, Auxiliary Integrals, Heat Transfer and Friction Coefficients for Fully Developed Mixing Profiles. University of Illinois, ME-TN-392-4, Contract No. AF 18(600)392, January 1959.

8. Shapiro, A. H., The Dynamics and Thermodynamics of Compressible Fluid Flow, Volume I, April 1953, pp. 533.

9. Dailey, C. L., and Wood, F. C., Computation Curves for Compressible Fluid Problems. John Wiley & Sons, Inc., 1949.

10. NACA Report 1135, Equations, Tables, and Charts for Compressible Flow, 1953.

11. Korst, H. H., Chow, W. L., and Zumwalt, G. W., Research on Transonic and Supersonic Flow of a Real Fluid at Abrupt Increases in

Cross Section. (Final Report). Univ. of Illinois, ME-TN-392-5, Contract No. AF 18(600)-392, December 1959.

12. Love, E. S., <u>Base Pressure at Supersonic Speeds on Two-Dimensional Airfoils and on Bodies of Revolution with and Without Fins Having Turbulent Boundary Layers.</u> NACA TN-3819 Report, January 1957.

13. Lord, W. T., <u>A Theoretical Study of Annular Supersonic Nozzles.</u> Royal Aircraft Establishment, Report Aero. 2727, Ministry of Aviation, London, October 1959.

14. <u>Base Pressure Cylinder After-Body.</u> Rand Corporation, RM 1544, 1955 (Classified).

15. <u>Results of the Computation of Supersonic Flow Fields Aft of Circular Cylindrical Bodies of Revolution by the Method of Characteristics.</u> Report No. DA-R-49, March 1958, Redstone Arsenal, Alabama.

16. <u>Supersonic Flow Around Right Circular Cones, Tables for Zero Angle of Attack.</u> Report No. DA-TR-11-60, Army Ballistic Missile Agency, Redstone Arsenal, Alabama, March 1960.

17. <u>IBM Problem M Curves.</u> Technical Memorandum SCTM 268-56-51, the Sandia Corporation, Reprinted June 1960.

18. Reller, J. O., Jr. and Hamaker, F. M. <u>An Experimental Investigation of the Base Pressure Characteristics of Non-lifting Bodies of Revolution at Mach Numbers from 2.73 to 4.98.</u> NACA TN 3393, March 1955. (Supercedes RM A 52E20)

19. Chapman, D. R., <u>An Analysis of Base Pressure at Supersonic Velocities and Comparison with Experiments.</u> NACA Report 1051, 1951.

20. Liepmann, H. W. and Laufer, J. <u>Investigations On Free Turbulent Mixing.</u> NACA TN 1257, 1947.

21. Gooderum, P. B., Wood, G. P., and Brevoort, M. J., <u>Investigations with an Interferometer of the Turbulent Mixing of a Free Supersonic Jet.</u> NACA Report 963, 1950.

22. Bershader, D., and Pai, S. I. <u>On Turbulent Jet Mixing in Two-Dimensional Supersonic Flow.</u> Journal of Applied Physics, Vol. 21, No. 6, 1950, pp. 616.

23. Cary, B. <u>An Optical Study of Two-Dimensional Jet Mixing.</u> Ph.D. Thesis, University of Maryland, 1954.

APPENDIX 1

CALCULATION OF BASE PRESSURE FOR TWO-DIMENSIONAL, TURBULENT, STEADY FLOW

①	②	③	④	⑤	⑥	⑦	⑧	⑨	⑩
C_2^2	M_2	φ_j	C_d^2	$\dfrac{1}{(1-C_d^2)^{3.5}}$	$_3\theta_4$	ν_2	ν_1	M_1	$\dfrac{P_b}{P_1}$
				(P_4/P_3)			$(\nu_2 - _3\theta_4)$		
.36	1.677	.6405	.1480	1.75	11.25	17.15	5.90	1.290	.5575
.44	1.982	.6475	.1845	2.04	13.70	25.90	12.20	1.509	.4880
.52	2.327	.6554	.2235	2.42	15.45	36.10	20.65	1.789	.4200
.60	2.739	.6646	.2650	2.94	17.00	44.47	27.50	2.041	.3380
.68	3.260	.6755	.3108	3.68	18.20	55.04	36.84	2.405	.2730
.76	3.979	.6890	.3612	4.80	18.80	65.51	46.70	2.847	.1970
.84	5.124	.7069	.4200	6.73	19.00	78.05	59.05	3.532	.1313
.88	6.052	.7190	.4550	8.35	18.60	85.33	66.73	4.073	.1010
.92	7.585	.7310	.4920	10.73	17.80	93.83	76.00	4.900	.0679
.95	9.500	.7430	.5244	13.40	15.93	100.89	84.96	6.000	.0523
.97	12.700	.7540	.5515	16.53	13.35	108.15	94.80	7.805	.0393

WORK SHEET FOR BLAST WAVE PASSING TWO-DIMENSIONAL
BODY AXIALLY HEAD-ON

Altitude	$M_{\infty x}$	ΔP_{max}	$P_{\infty x}$	$T_{\infty x}$	Wedge Half Angle	$a_{\infty x}$
30,000 ft	2	3 Psia	6.754 Psia	448°R	$\delta = 10°$	1037 FPS

x = before shock
y = immediately after
    shock passes

Condition x:

$$U_{\infty x} = a_{\infty x} M_{\infty x} = 2074 \text{ FPS.} \qquad \left.\frac{P_{\infty x}}{P_{0_{\infty x}}}\right|_{M_{\infty x}} = .1278$$

Oblique shock on
Nose, for $M_{\infty x}$ and δ : $M_{fx} = 1.64$; $\nu_{fx} = 16.05$; $\dfrac{P_{0_{1x}}}{P_{0_{\infty x}}} = .986$

$$\nu_{1x} = \nu_{fx} + \delta = 26.05 \rightarrow M_{1x} = 1.988, \text{ and } \frac{P_{1x}}{P_{0_{1x}}} = .13$$

$$\frac{P_{1x}}{P_{\infty x}} = \frac{\dfrac{P_{1x}}{P_{0_{1x}}} \times \dfrac{P_{0_{1x}}}{P_{0_{\infty x}}}}{\dfrac{P_{\infty x}}{P_{0_{\infty x}}}} = \frac{.13 \times .986}{.1278} = 1.003$$

$$\left.\frac{P_{bx}}{P_{1x}}\right|_{M_1} = .355 \quad ; \quad \frac{P_{bx}}{P_{0_{1x}}} = \frac{P_{bx}}{P_{1x}} \times \frac{P_{1x}}{P_{0_{1x}}} = .355 \times .13 = .04615$$

$$\therefore M_{2x} = 2.654 \; ; \quad \nu_{2x} = 42.60$$

$$\theta_x = \nu_{2x} - \nu_{1x} = 16.55$$

$$P_{bx} = \frac{P_{bx}}{P_{1x}} \times \frac{P_{1x}}{P_{\infty x}} \times P_{\infty x} = .355 \times 1.003 \times 6.754 = 2.4048 \text{ psia}$$

Condition y: $\quad P_{\infty y} = P_{\infty x} + \Delta P_{max} = 9.754$ psia

$$\frac{P_{\infty y}}{P_{\infty x}} = \frac{9.754}{6.754} = 1.4442$$

$$U_s = a_x \sqrt{\frac{6}{7} \frac{P_{\infty y}}{P_{\infty x}} + \frac{1}{7}}$$

$$= 1037 \sqrt{\frac{6 \times 1.4442 + 1}{7}} = 1218.5$$

$$U_y' = M_y'\left(a_{\infty x} \frac{a_{\infty y}}{a_{\infty x}}\right) = .8582 \times 1037 \times 1.055 = 938.9; \quad \left(a_{\infty y} = 1094 \, fps\right)$$

$$U_{\infty y} = U_{\infty x} + U_s - U_y' = 2074 + 1218.5 - 939 = 2354$$

$$M_{\infty y} = \frac{U_{\infty y}}{a_{\infty y}} \times \frac{a_{\infty x}}{a_{\infty y}} = \frac{2354}{1037} \times \frac{1}{1.055} = 2.152 \longrightarrow \frac{P_{\infty y}}{P_{o\infty y}} = .1000$$

Obique shock on
Nose for $M_{\infty y}$ and δ: $\quad M_{fy} = 1.78; \quad \mathcal{V}_{fy} = 20.15; \quad \frac{P_{o1y}}{P_{o\infty y}} = .983$

$$\mathcal{V}_{1y} = \mathcal{V}_{fy} + \delta = 30.15 \longrightarrow M_{1y} = 2.139; \quad \frac{P_{1y}}{P_{o1y}} = .1025$$

$$\frac{P_{1y}}{P_{\infty y}} = \frac{(P_{1y}/P_{o1y})(P_{o1y}/P_{o\infty y})}{(P_{\infty y}/P_{o\infty y})} = \frac{.1025 \times .983}{.1000} = 1.007;$$

$$\frac{P_{\infty y}}{P_{o1y}'} = \frac{P_{\infty y}}{P_{\infty x}} \times \frac{P_{\infty x}}{P_{o\infty y}} = 1.4442 \times .4281 = .6182; \quad \sqrt{T_{\infty y}} = \frac{a_{\infty y}}{a_{\infty x}} \sqrt{T_{\infty x}} = 2233$$

Stable y Solution:

$$\left.\frac{P_b}{P_1}\right|_{M_{1y}} = 0.326$$

$$P_{by(stabe)} = \frac{P_b}{P_1} \times \frac{P_{1y}}{P_{\infty y}} \times P_{\infty y} = .326 \times 1.007 \times 9.754 = 3.202 \, psia$$

Trial and Error Solution for P_{by}: $\quad \mathcal{V}_1 = 30.15; \quad \theta_x = 16.55; \quad P_{bx} = 2.4048$

$$\theta_y = 18.62; \quad \mathcal{V}_{2y} = \mathcal{V}_1 + \theta_y = 48.77 \longrightarrow \frac{P_{2y}}{P_{o1y}} = .294$$

$$P_{by} = P_{bx}\left(\frac{Tan \, \theta_y}{Tan \, \theta_x}\right)^{1.4} = 2.4048 \left(\frac{.33693}{.29147}\right)^{1.4} = 2.804$$

$$\therefore M_{2y} = 2.949; \quad P_{o1y} = \frac{P_{o1y}}{P_{o\infty y}} \times \frac{P_{\infty y}}{\frac{P_{\infty y}}{P_{o\infty y}}} = .983 \times \frac{9.754}{.100} = 95.88$$

APPENDIX 3

TRANSIENT BLAST WAVE PASSING TWO-DIMENSIONAL BASE

(SEE PICTURE IN APPENDIX 2.)

Based on Equations 5 and 6.

①. t

②. P_b, ② above + ⓔ x ㊾ , where ⓔ = Δt

③. P'_∞ , $P'_\infty = P_{\infty x} + \Delta P_t$, where ΔP_t obtained from equation 6

④. $\dfrac{P'_\infty}{P'_{o \infty y}}$, ③ x $\dfrac{ⓑ}{ⓐ}$, where ⓐ = $P_{\infty y}$; ⓑ = $\dfrac{P_{\infty y}}{P'_{o\infty y}}$

⑤. M' , ④ → ⑤ by isentropic relation (10).

⑥. $\left(\dfrac{P_\infty}{P_{\infty y}} \right)^{0.143}$, $\left(\dfrac{③}{ⓐ} \right)^{0.143}$

⑦. a_∞ , ⓒ x ⑥ , where ⓒ = $a_{\infty y}$

⑧. u'_∞ , ⑤ x ⑦

⑨. u_∞ , ⓓ — ⑧ , where ⓓ = $u_{body} + u_{shock}$

⑩. M_∞ , ⑨ / ⑦

⑪. $P_\infty / P_{o\infty}$, ⑩ — ⑪ isentropic relation (10).

⑫. $T_\infty / T_{o\infty}$, ⑩ — ⑫ isentropic relation (10).

⑬. M_f , ⑩ and δ (given) → ⑬ by oblique shock curves (9).

⑭. $P_1 / P_{o\infty}$, ⑩ and δ (given) → ⑭ by oblique shock curves (9).

⑮. ν_f , ⑬ — ⑮ by Prandtl-Meyer relations (10).

⑯. $\nu_1 = \nu_f + \delta$, ⑮ + δ

⑰. M_1 , ⑯ → ⑰ by Prandtl-Meyer relations (10).

⑱. P_1 / P_{o1} , ⑰ → ⑱ by isentropic relation (10).

⑲. P_1 / P_∞ , ⑱ x ⑭ / ⑪

(20) . P_b/P_1 (Stable), (17) → (20) from Figure 8

(21) . P_b (Stable), (19) x (20) x (3)

(22) . P_b/P_{01}, (2) x (18) / (3) x (19)

(23) . M_2, (22) → (23) by isentropic relation (10).

(24) . ν_2, (22) → (24) by isentropic relation, (10).

(25) . $_1\theta_2 = \nu_2 - \nu_1$, (24) — (16)

(26) . $\sin_1\theta_2$

(27) . $\tan_1\theta_2$

(28) . $c_2^2 = \dfrac{M_2^2}{5+M_2^2}$, $\dfrac{(23)^2}{5+(23)^2}$

(29) . I_j, (28) — (29) from Figure 5(a)

(30) . P_4/P_3, [(23) and (25)] → (30)

(31) . $c_d^2 = 1 - \dfrac{1}{\left(\frac{P_4}{P_3}\right)^{0.286}}$, $1 - \dfrac{1}{(30)^{0.286}}$

(32) . $\phi_d = \sqrt{\dfrac{c_d^2}{c_2^2}}$, $\sqrt{\dfrac{(31)}{(28)}}$

(33) . I_d, (28) and (32) — (33) from Figure 5(b).

(34) . P_{01}, $\dfrac{(14)\times(3)}{(11)}$

(35) . $\sqrt{T_\infty} = \dfrac{\sqrt{T_{\infty y}}}{a_{\infty y}} \times a_\infty$, $\dfrac{(f)}{(c)}$ x (7), where (f) $= \sqrt{T_{y\infty}}$

(36) . $\sqrt{T_{01}} = \dfrac{\sqrt{T_\infty}}{\sqrt{\frac{T_\infty}{T_{0\infty}}}}$, $\dfrac{(35)}{\sqrt{(12)}}$

(37) . $2.758 M_2$, 2.758 x 23

(38) . $_2 = 12 + 2.758 M_2$, 12 + (37)

(39) . c_2, $\sqrt{(28)}$

(40) . $1 - c_2^2$, 1 — (28)

(41) . $(1 - c_2^2)^{3.5}$, $(40)^{3.5}$

(42) . $\dfrac{P_{01} \times c_2(1-c_2^2)^{3.5}}{\sqrt{T_{01}}\ \bar{b}_2 \sin_1\theta_2}$, $\dfrac{(34)\times(39)\times(41)}{(36)\times(38)\times(26)}$

43. $I_j - I_d$, ㉙ — ㉝

44. G_d/h, $-296.1 \times$ ㊷ $\times$ ㊸, where $296.1 = 144\sqrt{\dfrac{2K}{R(K-1)}}$ and 144

is a converting factor of pressure unit.

45. Mass in the half wake, $\dfrac{P_b(\text{psia})}{T_1 \tan\theta} \times \dfrac{144}{R} = 1.35 \dfrac{②}{㉗ \times ㊱^2}$

46. $\dfrac{2 G_d P_b}{\text{Mass in wake}}$, $\dfrac{② \times ㊹ \times h}{㊺}$

47. $\dfrac{\text{Tan}\theta}{\text{Tan}\theta_{t+\triangle t}}$, choose and check by succeeding result of item ㉗

48. $\dfrac{\left[\dfrac{\text{Tan}\theta}{\text{Tan}\theta_{t+\triangle t}} - 1\right] P_b}{\triangle t}$, $\dfrac{\left[㊼ - 1\right] ②}{\triangle t}$

49. $\dfrac{2 G_d P_b}{\text{Mass in wake}} - \dfrac{\left[\dfrac{\text{Tan}\theta}{\text{Tan}\theta_{t+\triangle t}} - 1\right] P_b}{\triangle t}$, ㊻ — ㊽

VITA

HOMER HO TANG

Candidate for the Degree of

Master of Science

Thesis: ANALYTICAL STUDY OF HIGHLY TRANSIENT BASE PRESSURES AT SUPER-
SONIC SPEEDS

Major Field: Mechanical Engineering (Aeronautical)

Biographical:

Personal Data: Born in Swatow, Kwangtung, China, April 4, 1934,
the son of Jen and Shuh-Teh Tang.

Education: Attended public school in Kwangtung, China; graduated
from Taiwan Provincial Pingtung High School, China, 1951;
received the Bachelor of Science Degree in Mechanical Engi-
neering in June, 1956, from Taiwan Provincial Cheng-Kung
University, China; completed requirements for the Master of
Science Degree at Oklahoma State University, U.S.A., in
July, 1961.

Professional Experience: Served two years as a Second Lieutenant
with the Chinese Air Force, 1956-58; employed as Junior
Engineer at Taiwan Power Company, 1959-60; worked as a
Graduate Assistant at Oklahoma State University, 1960-61.